

# Big Data e Inteligencia Artificial: del concepto a la clínica

Ignacio Hernández Medrano

27 de marzo de 2019

# Machine Learning: Google Translate Example

The screenshot shows the Google Translate interface on a mobile device. At the top, the status bar displays 'AT&T LTE', '6:35 PM', and '40%' battery. Below the status bar, the language selection menu is open, showing 'English' on the left and 'Chinese (Sim...)' on the right, with a double-headed arrow icon between them. The input text 'Thank you for inviting me to the meeting' is entered in the English field. Below the input, there are icons for voice input (a microphone) and handwriting input (a stylized '2' or 'S' shape). The output is displayed in a blue box with white text: '谢谢你邀请我参加会议' (Xìexiè nǐ yāoqǐng wǒ cānjiā huìyì) and a speaker icon for audio playback.

●●○○ AT&T LTE 6:35 PM ↗ 40% 🔋

English ↔ Chinese (Sim...)

Thank you for inviting me to the meeting ×

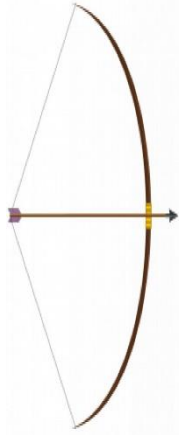
🎤 ✍️

谢谢你邀请我参加会议 🔊  
Xìexiè nǐ yāoqǐng wǒ cānjiā huìyì



# explosión big data



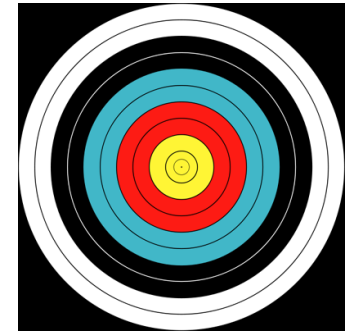


Sabes que sabes  
Determinista

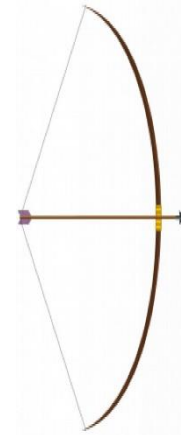
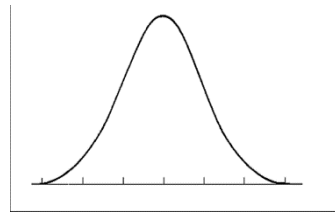
$$F = m \cdot a$$

↓   ↓   ↓

$$N = Kg \cdot \frac{m}{s^2}$$



Sabes que no  
sabes  
Probabilista  
(estocástico)



No sabes que no  
sabes  
Machine learning



# Computers cycles

1 - arithmetic and storing data



2 - connection



3 - shift place and time



4 - prediction



# The dramatic rise of the term "deep learning" in research

25,000 publications

20

15

10

5

0

'86 '88 '90 '92 '94 '96 '98 '00 '02 '04 '06 '08 '10 '12 '14 '16

Δ T L Δ S

| Data: [dimensions.ai](http://dimensions.ai)

# Machine Learning Algorithm Predicts Which New Faces Will Make It as Fashion Models

A machine-learning algorithm picks out the fashion models most likely to succeed.



(a) Fashion Model 1

(b) Fashion Model 4

(c) Fashion Model 6



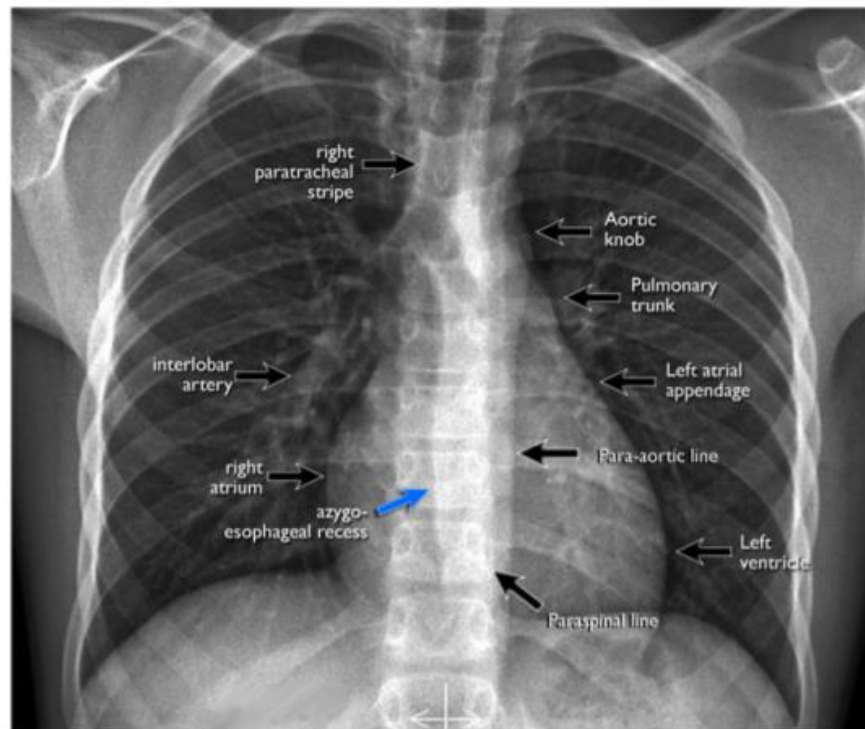
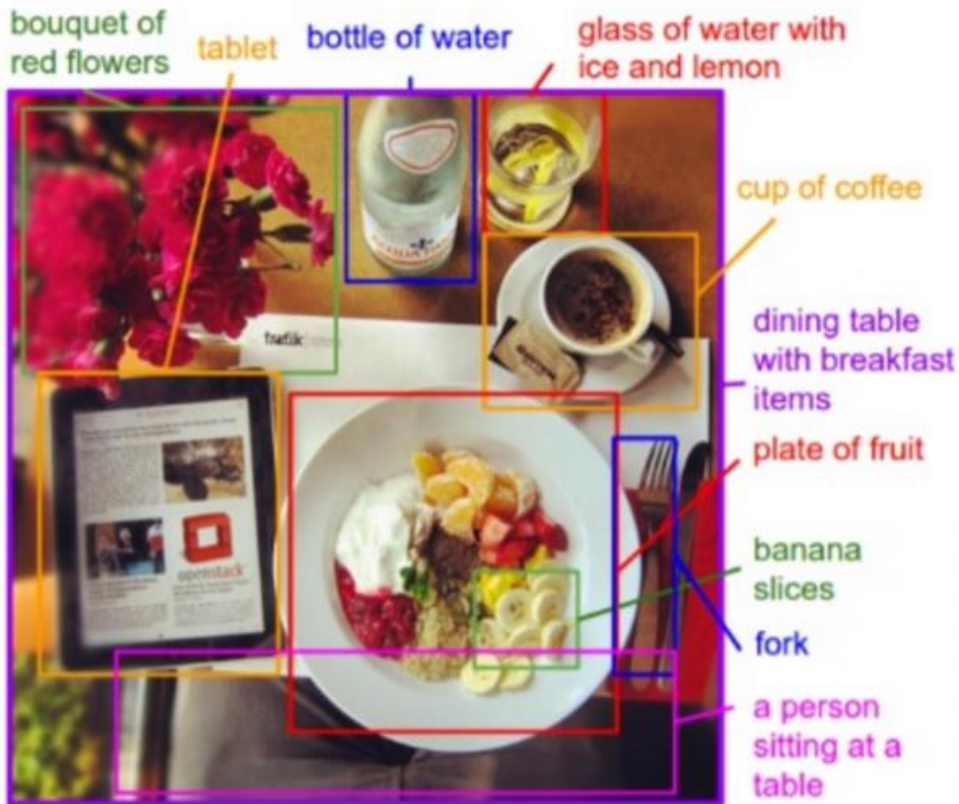


# Loro o guacamole



# Galleta o chihuahua





<http://www.radiologyassistant.nl/>

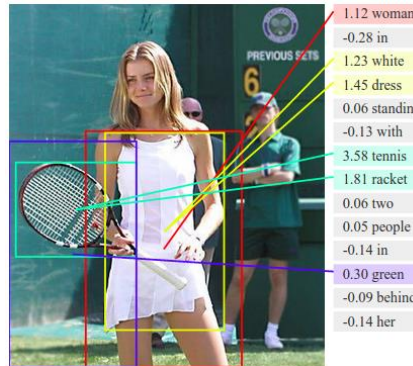
Karpathy, Andrej & Li, Fei Fei. Deep Visual-Semantic Alignments for Generating Image Descriptions, CVPR, 2015

## CLASIFICACIÓN



“perro”

## LOCALIZACIÓN



## RESUMEN



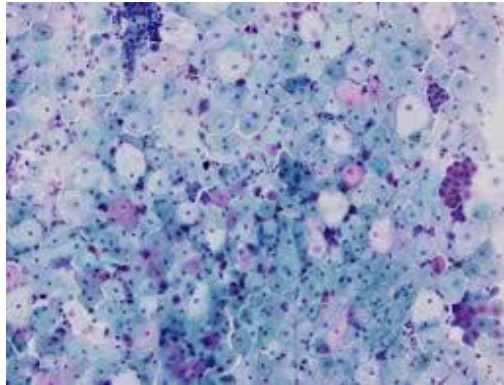
“un grupo de hombres jugando al fútbol”

## CLASIFICACIÓN



“benigno vs maligno”

## LOCALIZACIÓN



## RESUMEN



“fractura del húmero”

Original Investigation | Innovations in Health Care Delivery

FREE

December 13, 2016

# Development and Validation of a Deep Learning Algorithm for Detection of Diabetic Retinopathy in Retinal Fundus Photographs

Varun Gulshan, PhD<sup>1</sup>; Lily Peng, MD, PhD<sup>1</sup>; Marc Coram, PhD<sup>1</sup>; et al

[» Author Affiliations](#) | [Article Information](#)

JAMA. 2016;316(22):2402-2410. doi:10.1001/jama.2016.17216

# JAMA<sup>®</sup>

The Journal of the American Medical Association

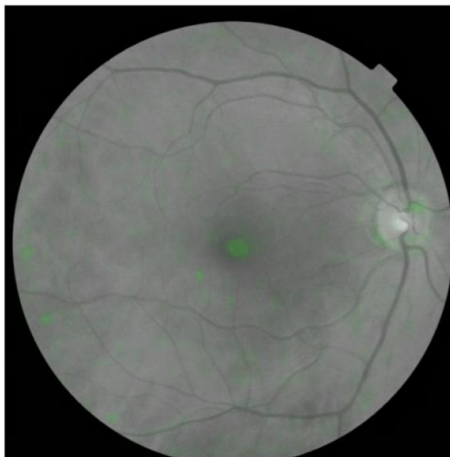
**FDA permits marketing of artificial intelligence-based device to detect certain diabetes-related eye problems**

FDA News Release

For Immediate Release



Gender



Actual: Female  
Predicted: Female

nature  
biomedical engineering

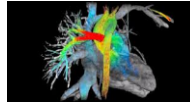
Article | Published: 19 February 2018

## Prediction of cardiovascular risk factors from retinal fundus photographs via deep learning

Ryan Poplin, Avinash V. Varadarajan, Katy Blumer, Yun Liu, Michael V. McConnell, Greg S. Corrado, Lily Peng [✉](#) & Dale R. Webster

*Nature Biomedical Engineering* 2, 158–164 (2018) | [Download Citation](#) ↓

Este documento ha sido descargado de la web del Club Excelencia en Gestión: [www.clubexcelencia.org](http://www.clubexcelencia.org)



Noviembre 17



Noviembre 17



Febrero 18



Abril 18



Mayo 18

# Automated and Clinical Breast Imaging Reporting and Data System Density Measures Predict Risk of Screen-Detected and Interval Cancers

Karla Kerlikowske, MD; Christopher G. Scott, MS; Amir P. Mahmoudzadeh, MScEng; Lin Ma, MS; Stacey Winham, PhD; Matthew R. Jensen, BS; Fang Fang Wu, BS; Serghei Malkov, PhD; V. Shane Pankratz, PhD; Steven R. Cummings, MD; John A. Shepherd, PhD; Kathleen R. Brandt, MD; Diana L. Miglioretti, PhD; and Celine M. Vachon, PhD



Home > Radiology > Recently Published

NEXT >

Original Research  
Thoracic Imaging

## Development and Validation of Deep Learning-based Automatic Detection Algorithm for Malignant Pulmonary Nodules on Chest Radiographs

Ju Gang Nam, Sunggyun Park, Eui Jin Hwang, Jong Hyuk Lee, Kwang-Nam Jin, Kun Young Lim, Thienkai Huy Vu, Jae Ho Sohn, Sangheum Hwang,

genotypes of genetic  
deep learning

Yaron Gurovich, Yair Hanani, Omri Bar, Guy Nadav, Nicole Fleischer, Dekel Gelbman, Lina Basel-Salmon, Peter M. Krawitz, Susanne B. Kamphausen, Martin Zenker, Lynne M. Bird & Karen W. Gripp

Nature Medicine 25, 60–64 (2019) | Download Citation

# Deep neural network improves fracture detection by clinicians

Robert Lindsey, Aaron Daluiski, Sumit Chopra, Alexander Lachapelle, Michael Mozer, Serge Sicular, Douglas Hanel, Michael Gardner, Anurag Gupta, Robert Hotchkiss, and Hollis Potter

PNAS published ahead of print October 22, 2018 <https://doi.org/10.1073/pnas.1806905115>

Edited by Terrence J. Sejnowski, Salk Institute for Biological Studies, La Jolla, CA, and approved September 14, 2018 (received for review April 25, 2018)

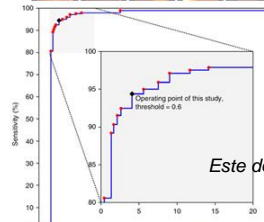
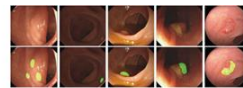


## ORIGINAL ARTICLE

OPEN

# Impact of Deep Learning Assistance on the Histopathologic Review of Lymph Nodes for Metastatic Breast Cancer

MD, PhD,\* Robert MacDonald, PhD,\* Yun Liu, PhD,\* Peter Truszkowski MD,\* p, MD, PhD, FCAP,\* Christopher Gammage, MS,\* Florence Thng, MS,† Lily Peng MD, PhD,\* and Martin C. Stumpe, PhD\*



Este documento ha sido descargado de la web del Club Excelencia en Gestión: [www.clubexcelencia.org](http://www.clubexcelencia.org)

**Stanford News**

Home Find Stories For Journalists Contact

NOVEMBER 15, 2017

### Stanford algorithm can diagnose pneumonia better than radiologists

Stanford researchers have developed a deep learning algorithm that evaluates chest X-rays for signs of disease. In just over a month of development, their algorithm outperformed expert radiologists at diagnosing pneumonia.

BY TAYLOR KUBOTA

Stanford researchers have developed an algorithm that offers diagnoses based off chest X-ray images. It can diagnose up to 14 types of medical conditions and is able to diagnose pneumonia better than expert radiologists working alone. A paper about the algorithm, called CheXNet, was published Nov. 14 on the open-access, scientific preprint website arXiv.

"Interpreting X-ray images to diagnose pathologies like pneumonia is very challenging, and we know that there's a lot of variability in the diagnoses radiologists arrive at," said Pranav Rajpurwalla, a graduate student in the Stanford Machine Learning Group and co-lead author of the paper.

**ARTICLES**  
biomedical engineering

**Development and validation of a deep-learning algorithm for the detection of polyps during colonoscopy**

Yu Wang\*, Xian-Ran\*, Jeremy R. Gibson Brown\*, Tyler M. Berenson\*, Mung-Hsi Tu\*, Fu-Kang\*, Xiao-Ni\*, Rui-Xia\*, Yan-Song\*, Di Zhang\*, Xue-Yang\*, Liang-Liang Li\*, Jang-Ho\*, Xin-Yi\*, Jing-Jin\* and Hong-Jin\*

The detection and removal of precancerous polyps via colonoscopy is the gold standard for the prevention of colorectal cancer. However, the detection of colon polyps can be difficult, especially for polyps smaller than 5 mm. We developed a deep learning algorithm for polyp detection that outperforms human experts. This algorithm was trained on 10,000 colonoscopy images and validated on 10,000 images. The algorithm achieved a sensitivity of 92% and a specificity of 90% for polyp detection. The algorithm was also evaluated on a separate dataset of 10,000 images and achieved a sensitivity of 91% and a specificity of 89% for polyp detection. The algorithm was also evaluated on a separate dataset of 10,000 images and achieved a sensitivity of 90% and a specificity of 88% for polyp detection. The algorithm was also evaluated on a separate dataset of 10,000 images and achieved a sensitivity of 89% and a specificity of 87% for polyp detection. The algorithm was also evaluated on a separate dataset of 10,000 images and achieved a sensitivity of 88% and a specificity of 86% for polyp detection. The algorithm was also evaluated on a separate dataset of 10,000 images and achieved a sensitivity of 87% and a specificity of 85% for polyp detection. The algorithm was also evaluated on a separate dataset of 10,000 images and achieved a sensitivity of 86% and a specificity of 84% for polyp detection. The algorithm was also evaluated on a separate dataset of 10,000 images and achieved a sensitivity of 85% and a specificity of 83% for polyp detection. The algorithm was also evaluated on a separate dataset of 10,000 images and achieved a sensitivity of 84% and a specificity of 82% for polyp detection. The algorithm was also evaluated on a separate dataset of 10,000 images and achieved a sensitivity of 83% and a specificity of 81% for polyp detection. The algorithm was also evaluated on a separate dataset of 10,000 images and achieved a sensitivity of 82% and a specificity of 80% for polyp detection. The algorithm was also evaluated on a separate dataset of 10,000 images and achieved a sensitivity of 81% and a specificity of 79% for polyp detection. The algorithm was also evaluated on a separate dataset of 10,000 images and achieved a sensitivity of 80% and a specificity of 78% for polyp detection. The algorithm was also evaluated on a separate dataset of 10,000 images and achieved a sensitivity of 79% and a specificity of 77% for polyp detection. The algorithm was also evaluated on a separate dataset of 10,000 images and achieved a sensitivity of 78% and a specificity of 76% for polyp detection. The algorithm was also evaluated on a separate dataset of 10,000 images and achieved a sensitivity of 77% and a specificity of 75% for polyp detection. The algorithm was also evaluated on a separate dataset of 10,000 images and achieved a sensitivity of 76% and a specificity of 74% for polyp detection. The algorithm was also evaluated on a separate dataset of 10,000 images and achieved a sensitivity of 75% and a specificity of 73% for polyp detection. The algorithm was also evaluated on a separate dataset of 10,000 images and achieved a sensitivity of 74% and a specificity of 72% for polyp detection. The algorithm was also evaluated on a separate dataset of 10,000 images and achieved a sensitivity of 73% and a specificity of 71% for polyp detection. The algorithm was also evaluated on a separate dataset of 10,000 images and achieved a sensitivity of 72% and a specificity of 70% for polyp detection. The algorithm was also evaluated on a separate dataset of 10,000 images and achieved a sensitivity of 71% and a specificity of 69% for polyp detection. The algorithm was also evaluated on a separate dataset of 10,000 images and achieved a sensitivity of 70% and a specificity of 68% for polyp detection. The algorithm was also evaluated on a separate dataset of 10,000 images and achieved a sensitivity of 69% and a specificity of 67% for polyp detection. The algorithm was also evaluated on a separate dataset of 10,000 images and achieved a sensitivity of 68% and a specificity of 66% for polyp detection. The algorithm was also evaluated on a separate dataset of 10,000 images and achieved a sensitivity of 67% and a specificity of 65% for polyp detection. The algorithm was also evaluated on a separate dataset of 10,000 images and achieved a sensitivity of 66% and a specificity of 64% for polyp detection. The algorithm was also evaluated on a separate dataset of 10,000 images and achieved a sensitivity of 65% and a specificity of 63% for polyp detection. The algorithm was also evaluated on a separate dataset of 10,000 images and achieved a sensitivity of 64% and a specificity of 62% for polyp detection. The algorithm was also evaluated on a separate dataset of 10,000 images and achieved a sensitivity of 63% and a specificity of 61% for polyp detection. The algorithm was also evaluated on a separate dataset of 10,000 images and achieved a sensitivity of 62% and a specificity of 60% for polyp detection. The algorithm was also evaluated on a separate dataset of 10,000 images and achieved a sensitivity of 61% and a specificity of 59% for polyp detection. The algorithm was also evaluated on a separate dataset of 10,000 images and achieved a sensitivity of 60% and a specificity of 58% for polyp detection. The algorithm was also evaluated on a separate dataset of 10,000 images and achieved a sensitivity of 59% and a specificity of 57% for polyp detection. The algorithm was also evaluated on a separate dataset of 10,000 images and achieved a sensitivity of 58% and a specificity of 56% for polyp detection. The algorithm was also evaluated on a separate dataset of 10,000 images and achieved a sensitivity of 57% and a specificity of 55% for polyp detection. The algorithm was also evaluated on a separate dataset of 10,000 images and achieved a sensitivity of 56% and a specificity of 54% for polyp detection. The algorithm was also evaluated on a separate dataset of 10,000 images and achieved a sensitivity of 55% and a specificity of 53% for polyp detection. The algorithm was also evaluated on a separate dataset of 10,000 images and achieved a sensitivity of 54% and a specificity of 52% for polyp detection. The algorithm was also evaluated on a separate dataset of 10,000 images and achieved a sensitivity of 53% and a specificity of 51% for polyp detection. The algorithm was also evaluated on a separate dataset of 10,000 images and achieved a sensitivity of 52% and a specificity of 50% for polyp detection. The algorithm was also evaluated on a separate dataset of 10,000 images and achieved a sensitivity of 51% and a specificity of 49% for polyp detection. The algorithm was also evaluated on a separate dataset of 10,000 images and achieved a sensitivity of 50% and a specificity of 48% for polyp detection. The algorithm was also evaluated on a separate dataset of 10,000 images and achieved a sensitivity of 49% and a specificity of 47% for polyp detection. The algorithm was also evaluated on a separate dataset of 10,000 images and achieved a sensitivity of 48% and a specificity of 46% for polyp detection. The algorithm was also evaluated on a separate dataset of 10,000 images and achieved a sensitivity of 47% and a specificity of 45% for polyp detection. The algorithm was also evaluated on a separate dataset of 10,000 images and achieved a sensitivity of 46% and a specificity of 44% for polyp detection. The algorithm was also evaluated on a separate dataset of 10,000 images and achieved a sensitivity of 45% and a specificity of 43% for polyp detection. The algorithm was also evaluated on a separate dataset of 10,000 images and achieved a sensitivity of 44% and a specificity of 42% for polyp detection. The algorithm was also evaluated on a separate dataset of 10,000 images and achieved a sensitivity of 43% and a specificity of 41% for polyp detection. The algorithm was also evaluated on a separate dataset of 10,000 images and achieved a sensitivity of 42% and a specificity of 40% for polyp detection. The algorithm was also evaluated on a separate dataset of 10,000 images and achieved a sensitivity of 41% and a specificity of 39% for polyp detection. The algorithm was also evaluated on a separate dataset of 10,000 images and achieved a sensitivity of 40% and a specificity of 38% for polyp detection. The algorithm was also evaluated on a separate dataset of 10,000 images and achieved a sensitivity of 39% and a specificity of 37% for polyp detection. The algorithm was also evaluated on a separate dataset of 10,000 images and achieved a sensitivity of 38% and a specificity of 36% for polyp detection. The algorithm was also evaluated on a separate dataset of 10,000 images and achieved a sensitivity of 37% and a specificity of 35% for polyp detection. The algorithm was also evaluated on a separate dataset of 10,000 images and achieved a sensitivity of 36% and a specificity of 34% for polyp detection. The algorithm was also evaluated on a separate dataset of 10,000 images and achieved a sensitivity of 35% and a specificity of 33% for polyp detection. The algorithm was also evaluated on a separate dataset of 10,000 images and achieved a sensitivity of 34% and a specificity of 32% for polyp detection. The algorithm was also evaluated on a separate dataset of 10,000 images and achieved a sensitivity of 33% and a specificity of 31% for polyp detection. The algorithm was also evaluated on a separate dataset of 10,000 images and achieved a sensitivity of 32% and a specificity of 30% for polyp detection. The algorithm was also evaluated on a separate dataset of 10,000 images and achieved a sensitivity of 31% and a specificity of 29% for polyp detection. The algorithm was also evaluated on a separate dataset of 10,000 images and achieved a sensitivity of 30% and a specificity of 28% for polyp detection. The algorithm was also evaluated on a separate dataset of 10,000 images and achieved a sensitivity of 29% and a specificity of 27% for polyp detection. The algorithm was also evaluated on a separate dataset of 10,000 images and achieved a sensitivity of 28% and a specificity of 26% for polyp detection. The algorithm was also evaluated on a separate dataset of 10,000 images and achieved a sensitivity of 27% and a specificity of 25% for polyp detection. The algorithm was also evaluated on a separate dataset of 10,000 images and achieved a sensitivity of 26% and a specificity of 24% for polyp detection. The algorithm was also evaluated on a separate dataset of 10,000 images and achieved a sensitivity of 25% and a specificity of 23% for polyp detection. The algorithm was also evaluated on a separate dataset of 10,000 images and achieved a sensitivity of 24% and a specificity of 22% for polyp detection. The algorithm was also evaluated on a separate dataset of 10,000 images and achieved a sensitivity of 23% and a specificity of 21% for polyp detection. The algorithm was also evaluated on a separate dataset of 10,000 images and achieved a sensitivity of 22% and a specificity of 20% for polyp detection. The algorithm was also evaluated on a separate dataset of 10,000 images and achieved a sensitivity of 21% and a specificity of 19% for polyp detection. The algorithm was also evaluated on a separate dataset of 10,000 images and achieved a sensitivity of 20% and a specificity of 18% for polyp detection. The algorithm was also evaluated on a separate dataset of 10,000 images and achieved a sensitivity of 19% and a specificity of 17% for polyp detection. The algorithm was also evaluated on a separate dataset of 10,000 images and achieved a sensitivity of 18% and a specificity of 16% for polyp detection. The algorithm was also evaluated on a separate dataset of 10,000 images and achieved a sensitivity of 17% and a specificity of 15% for polyp detection. The algorithm was also evaluated on a separate dataset of 10,000 images and achieved a sensitivity of 16% and a specificity of 14% for polyp detection. The algorithm was also evaluated on a separate dataset of 10,000 images and achieved a sensitivity of 15% and a specificity of 13% for polyp detection. The algorithm was also evaluated on a separate dataset of 10,000 images and achieved a sensitivity of 14% and a specificity of 12% for polyp detection. The algorithm was also evaluated on a separate dataset of 10,000 images and achieved a sensitivity of 13% and a specificity of 11% for polyp detection. The algorithm was also evaluated on a separate dataset of 10,000 images and achieved a sensitivity of 12% and a specificity of 10% for polyp detection. The algorithm was also evaluated on a separate dataset of 10,000 images and achieved a sensitivity of 11% and a specificity of 9% for polyp detection. The algorithm was also evaluated on a separate dataset of 10,000 images and achieved a sensitivity of 10% and a specificity of 8% for polyp detection. The algorithm was also evaluated on a separate dataset of 10,000 images and achieved a sensitivity of 9% and a specificity of 7% for polyp detection. The algorithm was also evaluated on a separate dataset of 10,000 images and achieved a sensitivity of 8% and a specificity of 6% for polyp detection. The algorithm was also evaluated on a separate dataset of 10,000 images and achieved a sensitivity of 7% and a specificity of 5% for polyp detection. The algorithm was also evaluated on a separate dataset of 10,000 images and achieved a sensitivity of 6% and a specificity of 4% for polyp detection. The algorithm was also evaluated on a separate dataset of 10,000 images and achieved a sensitivity of 5% and a specificity of 3% for polyp detection. The algorithm was also evaluated on a separate dataset of 10,000 images and achieved a sensitivity of 4% and a specificity of 2% for polyp detection. The algorithm was also evaluated on a separate dataset of 10,000 images and achieved a sensitivity of 3% and a specificity of 1% for polyp detection. The algorithm was also evaluated on a separate dataset of 10,000 images and achieved a sensitivity of 2% and a specificity of 0% for polyp detection. The algorithm was also evaluated on a separate dataset of 10,000 images and achieved a sensitivity of 1% and a specificity of 0% for polyp detection. The algorithm was also evaluated on a separate dataset of 10,000 images and achieved a sensitivity of 0% and a specificity of 0% for polyp detection.

# Biología de sistemas... también exponencial

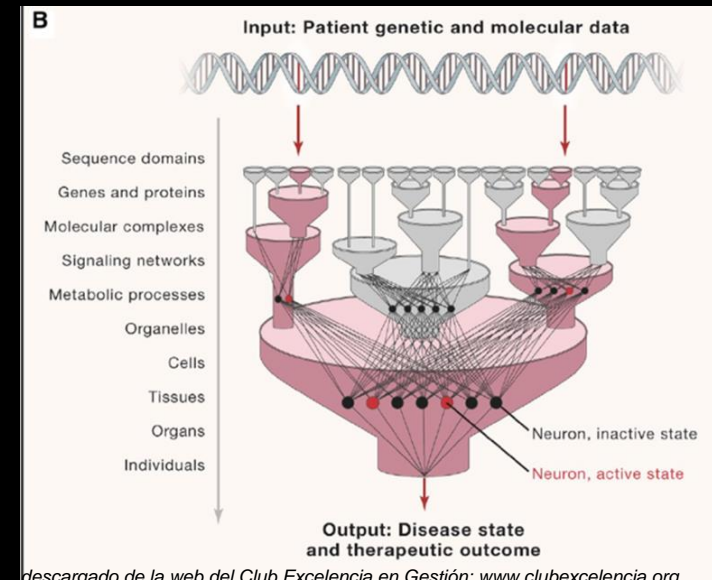
Exposoma: ?

Conectoma:  $10^{69}$

Proteoma:  $10^{20}$

Transcriptoma:  $10^{16}$

Genoma:  $10^9$





- AlQuraishi, M. End-to-end differentiable learning of protein structure. Preprint at <https://doi.org/10.1101/265231> (2018).
- Espinoza, J. L. Machine learning for tackling microbiota data and infection complications in immunocompromised patients with cancer. *J. Intern. Med.* <https://doi.org/10.1111/joim.12746> (2018).
- van Dijk, D. et al. Recovering gene interactions from single-cell data using data diffusion. *Cell* 174, 716–729.e727 (2018).
- Zitnik, M. et al. Machine learning for integrating data in biology and medicine: principles, practice, and opportunities. Preprint at <https://doi.org/10.1111/joim.12746> (2018).
- Camacho, D. M. et al. Next-generation machine learning for biological networks. *Cell* 173, 1581–1592 (2018).
- Kim, H. K. et al. Deep learning improves prediction of CRISPR–Cpf1 guide RNA activity. *Nat. Biotechnol.* 36, 239–241 (2018).
- Listgarten, J. et al. Prediction of off-target activities for the end-to-end design of CRISPR guide RNAs. *Nat. Biomed. Eng.* 2, 38–47 (2018).
- Caravagna, G. et al. Detecting repeated cancer evolution from multi-region tumor sequencing data. *Nat. Methods* 15, 707–714 (2018).
- Manak, M. et al. Live-cell phenotypic-biomarker microfluidic assay for the risk stratification of cancer patients via machine learning. *Nature Biomed. Eng.* 2, 761–772 (2018).
- Hassabis, D. et al. Neuroscience-inspired artificial intelligence. *Neuron* 95, 245–258 (2017).
- Robie, A. A. et al. Mapping the neural substrates of behavior. *Cell* 170, 393–406 e328 (2017).
- Dasgupta, S. et al. A neural algorithm for a fundamental computing problem. *Science* 358, 793–796 (2017).

- Januszewski, M. et al. High-precision automated reconstruction of neurons with flood-filling networks. *Nat. Methods* 15, 605–610 (2018).
- Savelli, F. & Knierim, J. J. AI mimics brain codes for navigation. *Nature* 557, 313–314 (2018).
- Banino, A. et al. Vector-based navigation using grid-like representations in artificial agents. *Nature* 557, 429–433 (2018).
- Adam, G. C. Two artificial synapses are better than one. *Nature* 558, 39–40 (2018).
- Wright, C. D. Phase-change devices: crystal-clear neuronal computing. *Nat. Nanotechnol.* 11, 655–656 (2016).
- Mathis, A. et al. DeepLabCut: markerless pose estimation of user-defined body parts with deep learning. *Nat. Neurosci.* 21, 1281–1289 (2018).
- Smalley, E. AI-powered drug discovery captures pharma interest. *Nat. Biotechnol.* 35, 604–605 (2017).
- Schneider, G. Automating drug discovery. *Nat. Rev. Drug. Discov.* 17, 97–113 (2018).
- Chakradhar, S. Predictable response: finding optimal drugs and doses using artificial intelligence. *Nat. Med.* 23, 1244–1247 (2017).
- Lowe, D. AI designs organic syntheses. *Nature* 555, 592–593 (2018).
- Luechtefeld, T. et al. Machine learning of toxicological big data enables read-across structure activity relationships (RASAR) outperforming animal test reproducibility. *Toxicol. Sci.* 165, 198–212 (2018).
- Hie, B. et al. Realizing private and practical pharmacological collaboration. *Science* 362, 347–350 (2018).
- Bilsland, E. et al. Plasmodium dihydrofolate reductase is a second enzyme target for the antimalarial action of triclosan. *Sci. Rep.* 8, 1038 (2018).

# Data infrastructure



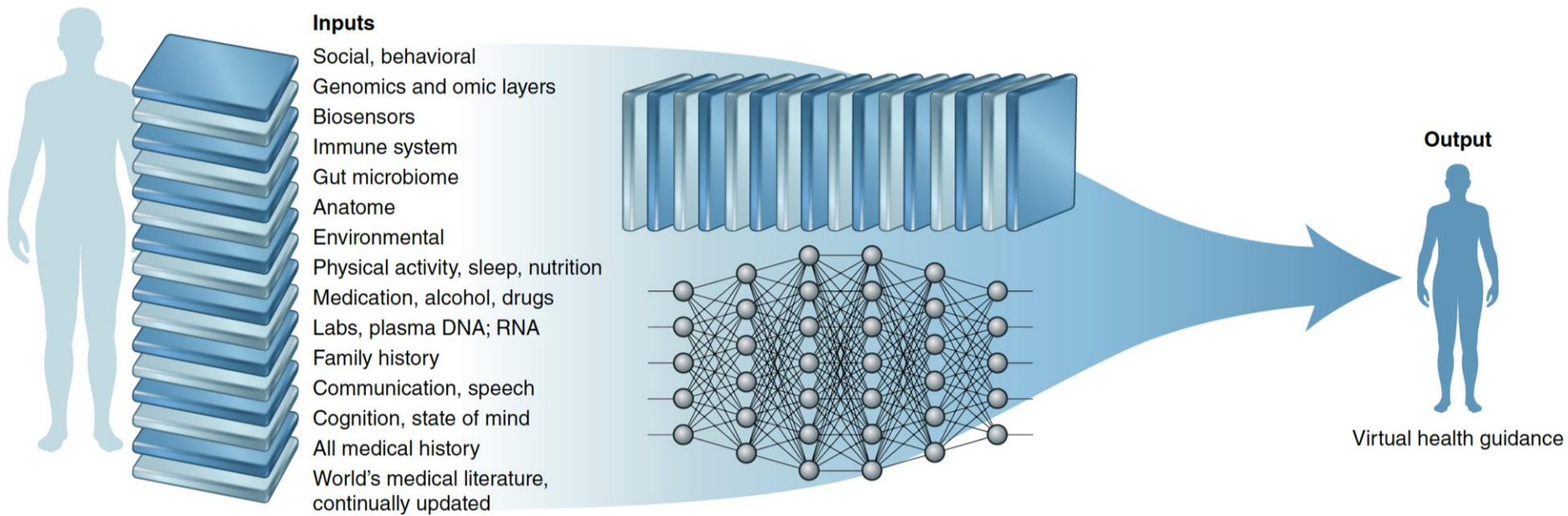
26.000 programadores

J.P.Morgan

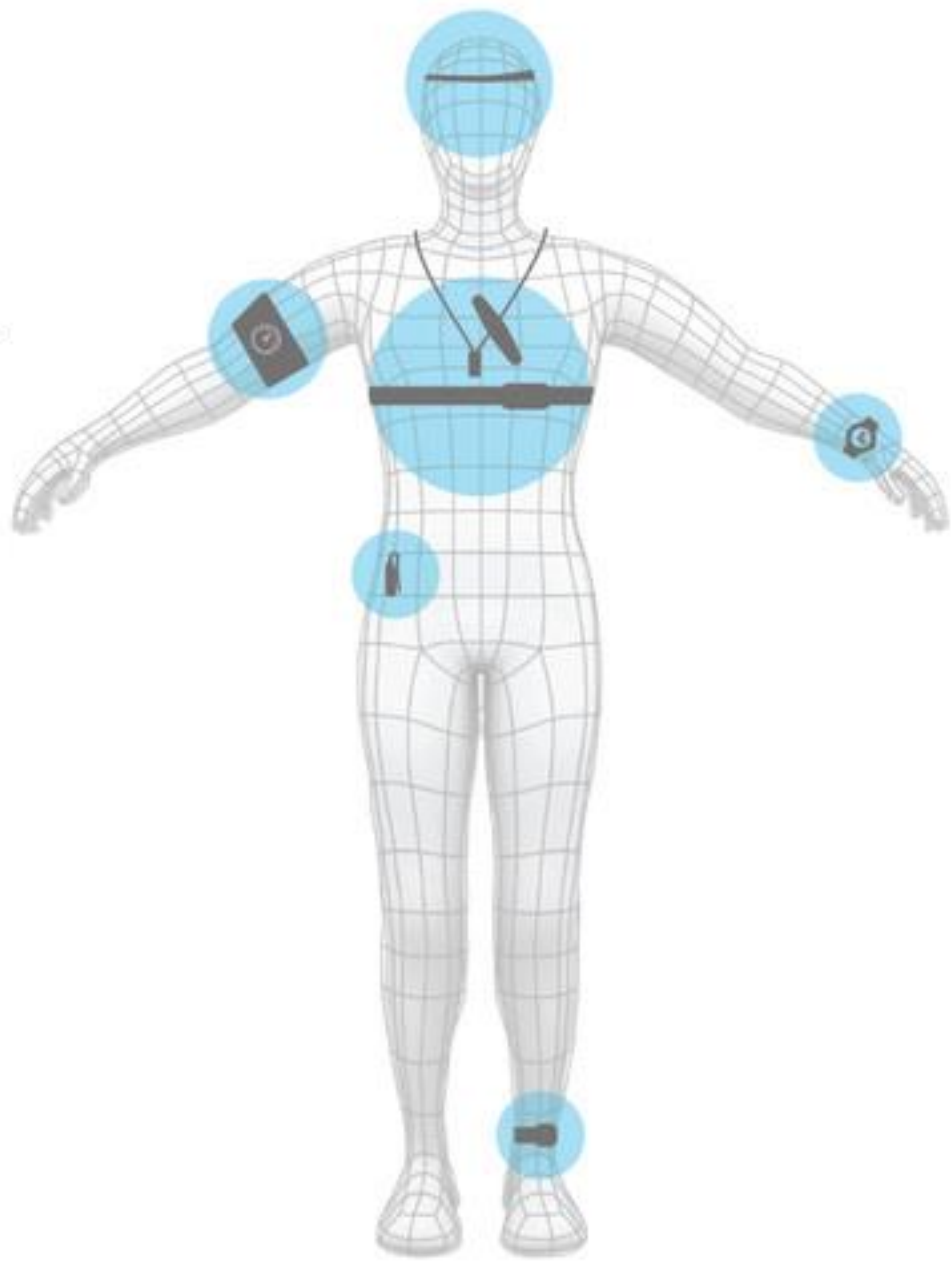
30.000 programadores

Healthcare information grows 48% / year

Accenture 2018



- Posture**  
Lumo  
Zephyr  
Jins Meme
- Muscle Activity**  
Athos
- Blood Pressure**  
iHealth  
Withings
- Skin Conductance**  
Basis  
Body Media  
Empatica  
Neumitra
- Movement**  
Fitbit  
Nike Fuelband  
Jawbone Up Band  
Garmin  
Samsung  
MC10  
Zephyr  
Withings  
Spire  
iHealth  
Jins Meme  
Proteus  
Neumitra  
Body Media  
Empatica  
Owlet
- Oxygen Level**  
iHealth  
Withings  
Owlet
- Hydration**  
Corventis  
MC10
- Temperature**  
Tempdrop  
MC10  
Empatica  
BodyMedia  
Basis  
Owlet



- Brain Activity**  
NeuroSky  
Melon (acquired by DAQR)  
Emotiv
- Glucose**  
Google  
Dexcom  
Glycens Incorporated
- Eye Tracking**  
Jins Meme
- Sleep**  
FitBit  
Rest Devices  
Garmin  
Nike  
Amigo  
BodyMedia  
Withings  
Samsung  
Misfit  
Jawbone  
iHealth  
Basis  
Owlet
- Respiration**  
Spire  
Zephyr  
Rest Devices
- Ingestion**  
Proteus
- Heart Tracking**  
Zephyr  
Withings  
Sprouting  
Proteus  
iHealth  
Basis  
Corventis  
AliveCor  
Samsung  
Garmin  
Empatica  
Owlet

\* This is not a comprehensive list



# Smartwatch Algorithm for Automated Detection of Atrial Fibrillation

Joseph M. Bumgarner, MD,<sup>2</sup> Cameron T. Lambert, MD,<sup>2</sup> Ayman A. Hussein, MD,<sup>2</sup> Daniel J. Cantillon, MD,<sup>2</sup> Bryan Baranowski, MD,<sup>2</sup> Kathy Wolski, MPH,<sup>2</sup> Bruce D. Lindsay, MD,<sup>2</sup> Oussama M. Wazni, MD, MBA,<sup>2</sup> Khalidoun G. Tarakji, MD, MPH<sup>1</sup>

**ABSTRACT**

**BACKGROUND** The Kardia Band (KB) is a novel technology that enables patients to record a rhythm strip using an Apple Watch (Apple, Cupertino, California). The band is paired with an app providing automated detection of atrial fibrillation (AF).

**OBJECTIVES** The purpose of this study was to examine whether the KB could accurately differentiate sinus rhythm (SR) from AF compared with physician-interpreted 12-lead electrocardiograms (ECGs) and KB recordings.

**METHODS** Consecutive patients with AF presenting for cardioversion (CV) were enrolled. Patients underwent pre-CV ECG along with a KB recording. If CV was performed, a post-CV ECG was obtained along with a KB recording. The KB interpretations were compared to physician-reviewed ECGs. The KB recordings were reviewed by blinded electrophysiologists and compared to ECG interpretations. Sensitivity, specificity, and K coefficient were measured.

**RESULTS** A total of 100 patients were enrolled (age  $68 \pm 11$  years). Eight patients did not undergo CV as they were found to be in SR. There were 169 simultaneous ECG and KB recordings. Fifty-seven were noninterpretable by the KB. Compared with ECG, the KB interpreted AF with 93% sensitivity, 84% specificity, and a K coefficient of 0.77. Physician interpretation of KB recordings demonstrated 99% sensitivity, 83% specificity, and a K coefficient of 0.83. Of the 57 noninterpretable KB recordings, interpreting electrophysiologists diagnosed AF with 100% sensitivity, 80% specificity, and a K coefficient of 0.74. Among 113 cases where KB and physician readings of the same recording were interpretable, agreement was excellent (K coefficient = 0.88).

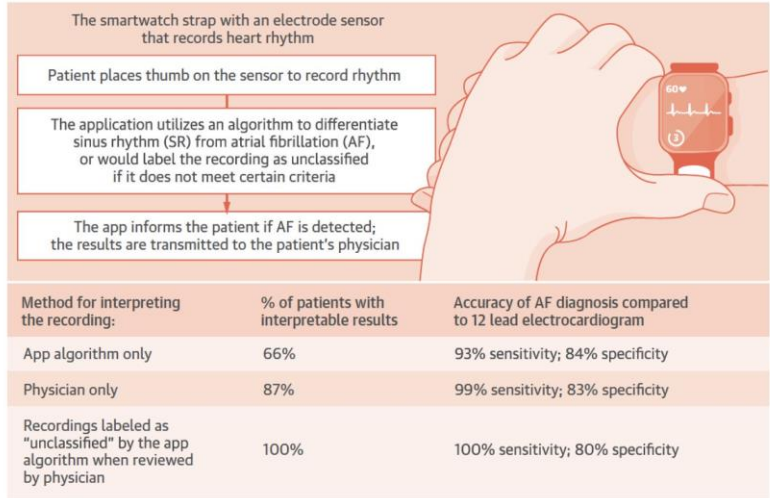
**CONCLUSIONS** The KB algorithm for AF detection supported by physician review can accurately differentiate AF from SR. This technology can help screen patients prior to elective CV and avoid unnecessary procedures. (J Am Coll Cardiol 2018;71:2381-8) © 2018 by the American College of Cardiology Foundation.

Atrial fibrillation (AF) is the most commonly encountered arrhythmia in clinical practice and population-based studies forecast over 6 million individuals living with this diagnosis by 2050 (1,2). It is a chronic condition whose prevalence increases with age, and represents a growing economic burden for our health care system (3,4). Although the journey of AF begins with an initial

<sup>1</sup> From the <sup>1</sup>Department of Cardiovascular Medicine, Cleveland Clinic, Cleveland, Ohio; and the <sup>2</sup>Cleveland Clinic Coordinating Center for Clinical Research (CCResearch), Cleveland Clinic, Cleveland, Ohio. AliveCor provided the Kardia Band monitors that were connected to an Apple Watch and paired via Bluetooth to a smartphone device for utilization in the study. AliveCor was not involved in the design, implementation, data analysis, or manuscript preparation of the study. Dr. Hussein has served as a consultant for Abbott and Biosense Webster. Dr. Cantillon has served as a consultant for Abbott, Boston Scientific, Stryker Sustainability, and LifeWatch. Dr. Wazni has received a speaker honorarium from Spectrametrics. Dr. Tarakji has served on the medical advisory board of Medtronic and AliveCor. All other authors have reported that they have no relationships relevant to the contents of this paper to disclose.

Manuscript received February 14, 2018; revised manuscript received March 1, 2018, accepted March 2, 2018.

**CENTRAL ILLUSTRATION** Automated Atrial Fibrillation Detection Algorithm Using Novel Smartwatch Technology

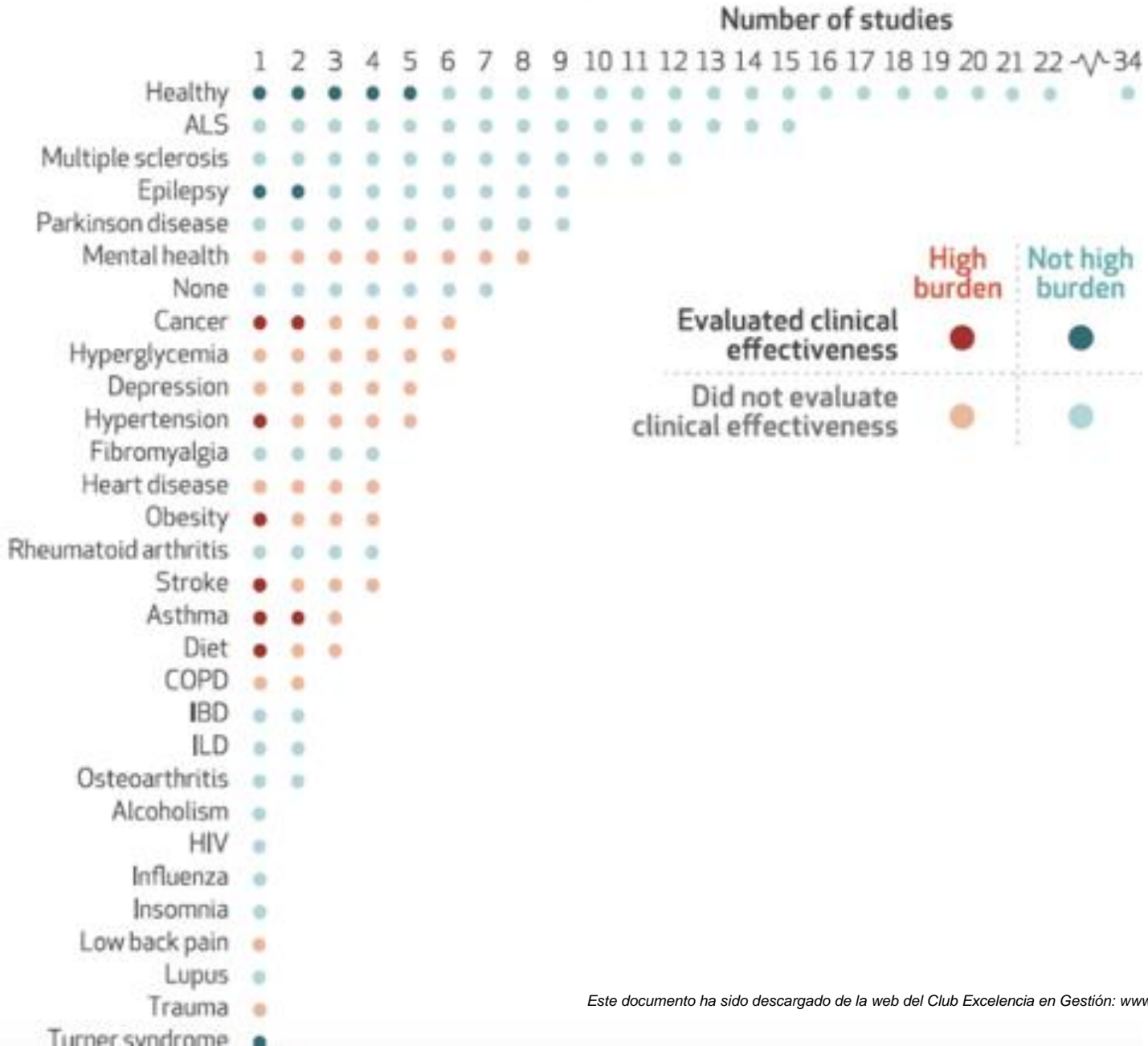


Bumgarner, J.M. et al. J Am Coll Cardiol. 2018;71(21):2381-8.

**FIGURE 1** The Kardia Band From AliveCor Paired With an Apple Smartwatch



# Studies by the twenty top-funded privately held US-based digital health companies, by burden level and clinical effectiveness and by population, condition, or risk factor

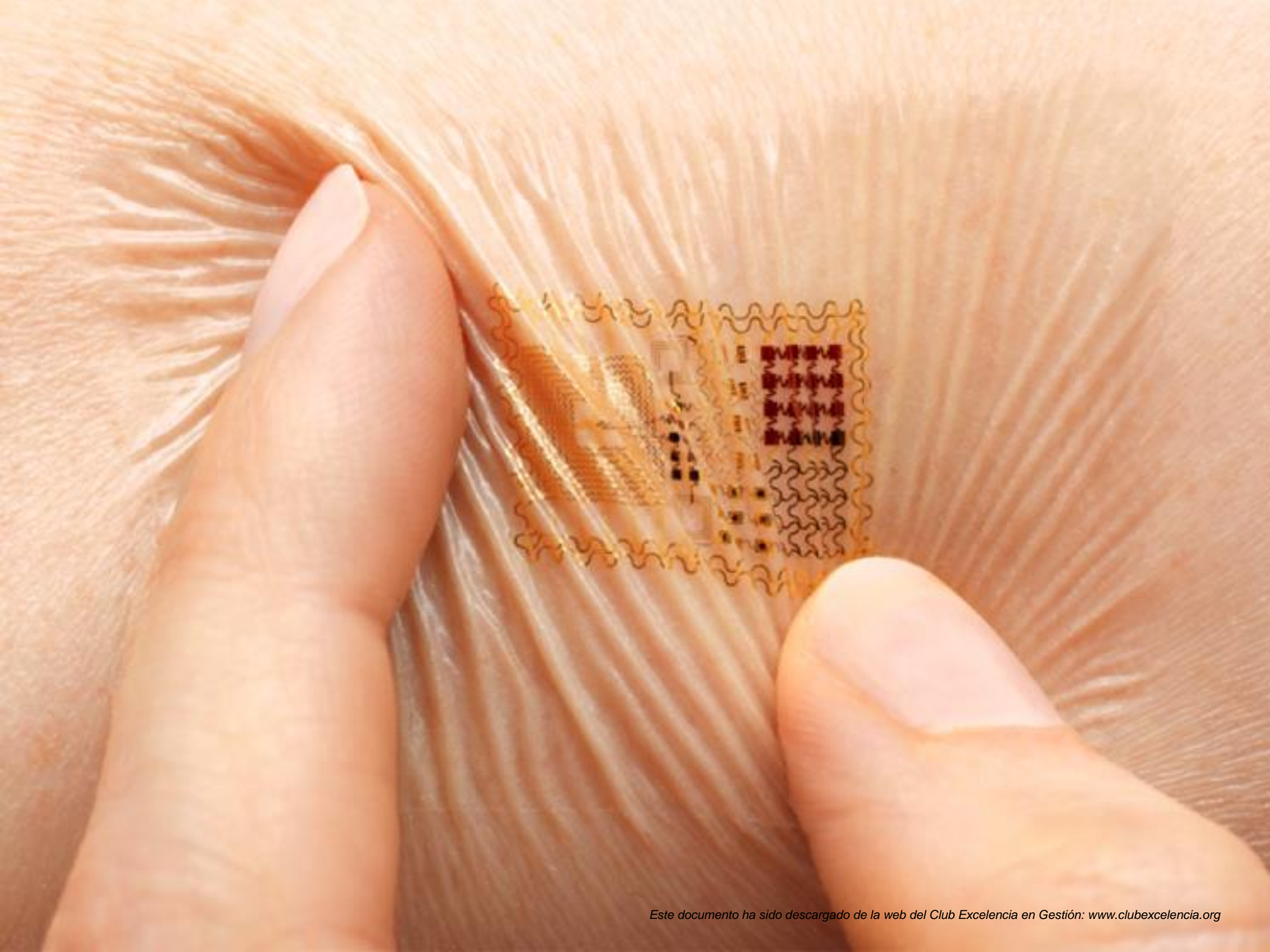




# Digital Medicine Clinical Trials

Condition	Digital Intervention	Impact	Citation
Asthma	Inhaler Sensor + GPS for hot spots	Reduce rescue inhaler use by 78%; 48% more symptom-free days (Louisville Air)	Barrett, Health Affairs, April 2018
Hypertension	Smartphone app RCT	Improved medication adherence	Morawski, JAMA Internal Med 2018
Diabetes	Telemedicine RCT	Improved control of Type 2 diabetes	Wild et al, PLOS Medicine, 2016
Heart failure	Telemedicine RCT	Less hospital admission and mortality	Koehler, Lancet, 2018
Inflammatory Bowel Disease	Telemedicine RCT	Striking reduction in outpatient visits and hospital admissions	De Jong, Lancet 2017
Cancer	Smartphone app RCT	Improved survival in lung cancer	Denis, ASCO 2018
Headaches	Telemedicine RCT	As effective as traditional consultations	Muller, Neurology, 2017
Visual Impairment	Smartphone app RCT	Marked improvement of detection among school children in Kenya	Rono, Lancet Global Health, 2018
Insomnia	Digital CBT RCT	Major reduction in insomnia among patients with mental health conditions	Freeman, Lancet Psychiatry, 2017
Attention deficit disorder	Video game RCT	Significant improvement of attention performance in children and adolescents	Kollins, December 2017 and Proof of Concept PLOS One, 2018
Schizophrenia	Avatar CBT RCT	Significant reduction of hallucinations	Craig, Lancet Psychiatry 2017

CBT-cognitive behavioral therapy, RCT-randomized controlled trial





[Home](#)

[Food](#)

[Drugs](#)

[Medical Devices](#)

[Radiation-Emitting Products](#)

[Vaccines, Blood & Biologics](#)

[Animal & Veterina](#)

## News & Events

[Home](#) > [News & Events](#) > [Newsroom](#) > [Press Announcements](#)

### FDA News Release

# FDA selects participants for new digital health software precertification pilot program

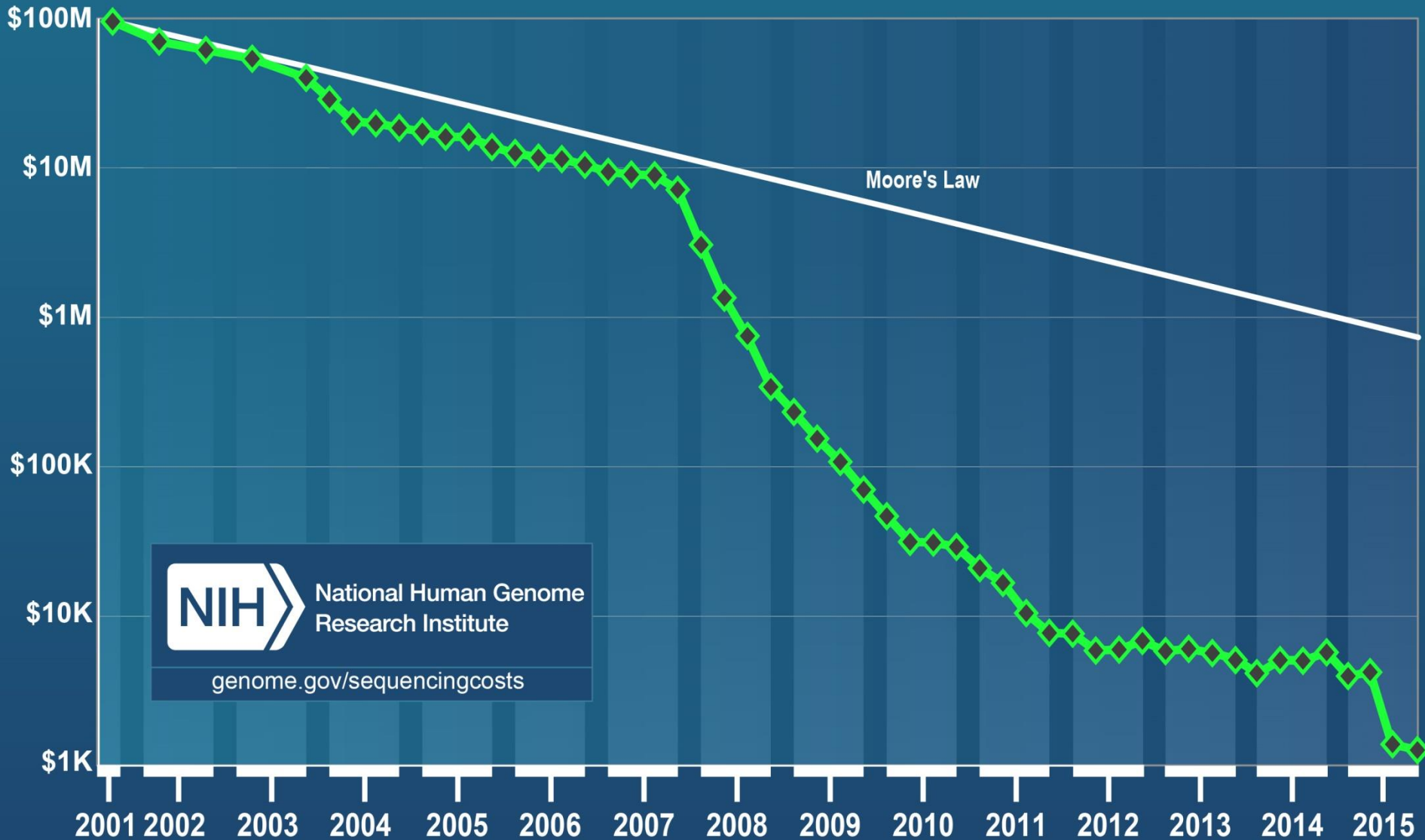
*Pilot program aims to advance the development of novel digital health applications*

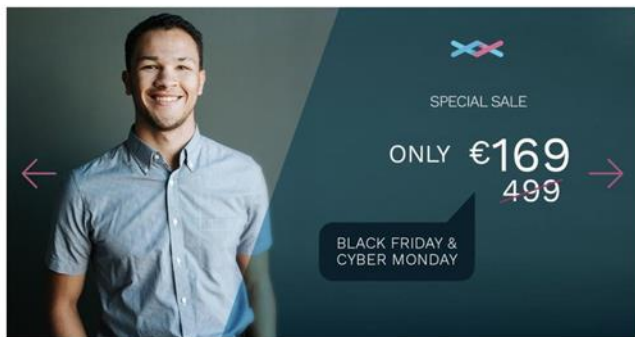
[f SHARE](#) [TWEET](#) [in LINKEDIN](#) [PIN IT](#) [EMAIL](#) [PRINT](#)

**For Immediate  
Release**

September 26, 2017

# Cost per Genome





## My Full DNA: Whole Genome Sequencing with mtDNA

€169.00 EUR ~~€850.00-EUR~~ You save €681.00 EUR

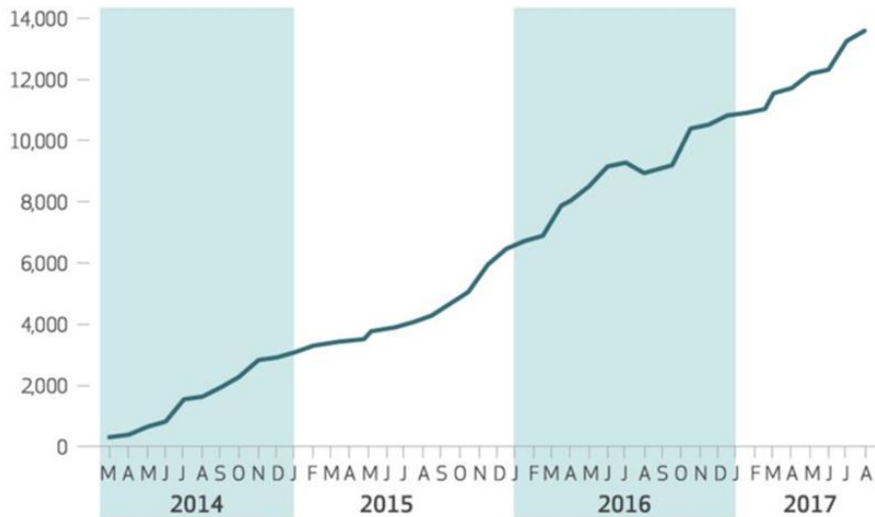
1 +  
-

ADD TO CART

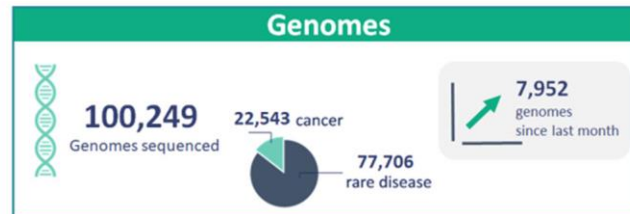
- Sample Customized Report on Genetic Diseases
- Sample Health & Wellness Report

### DESCRIPTION

Cumulative number of new genetic tests on the market, by month, March 2014–August 2017



Percentages of spending on genetic testing in six clinical domains, by quarter, 2014–16



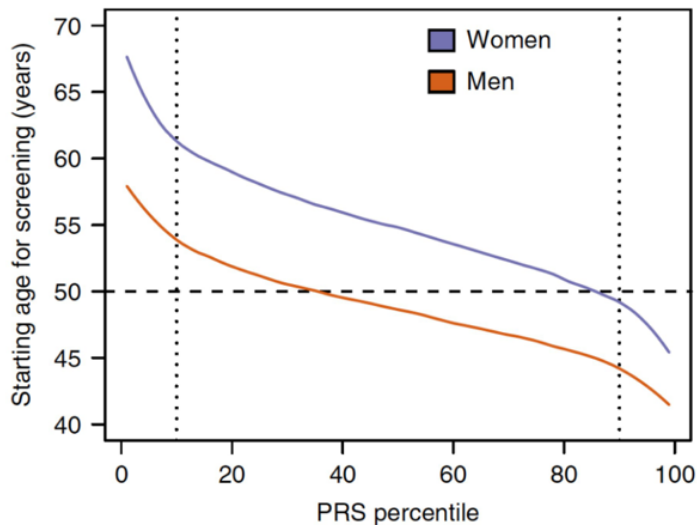
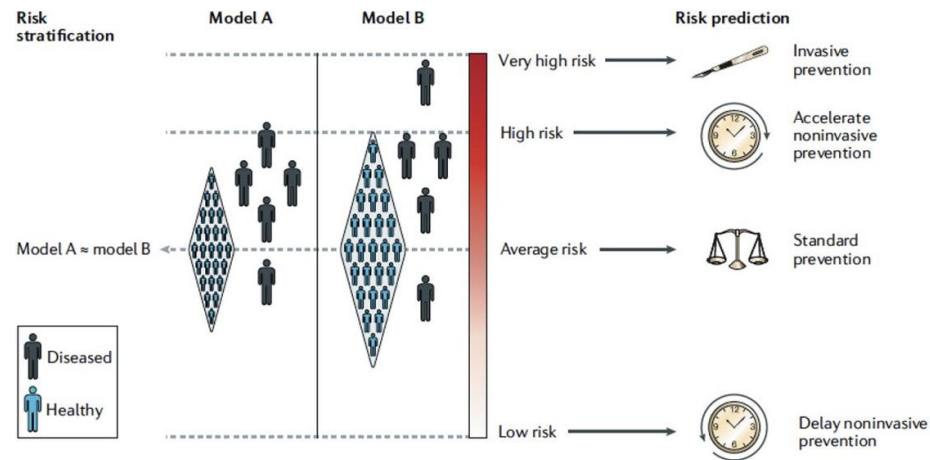


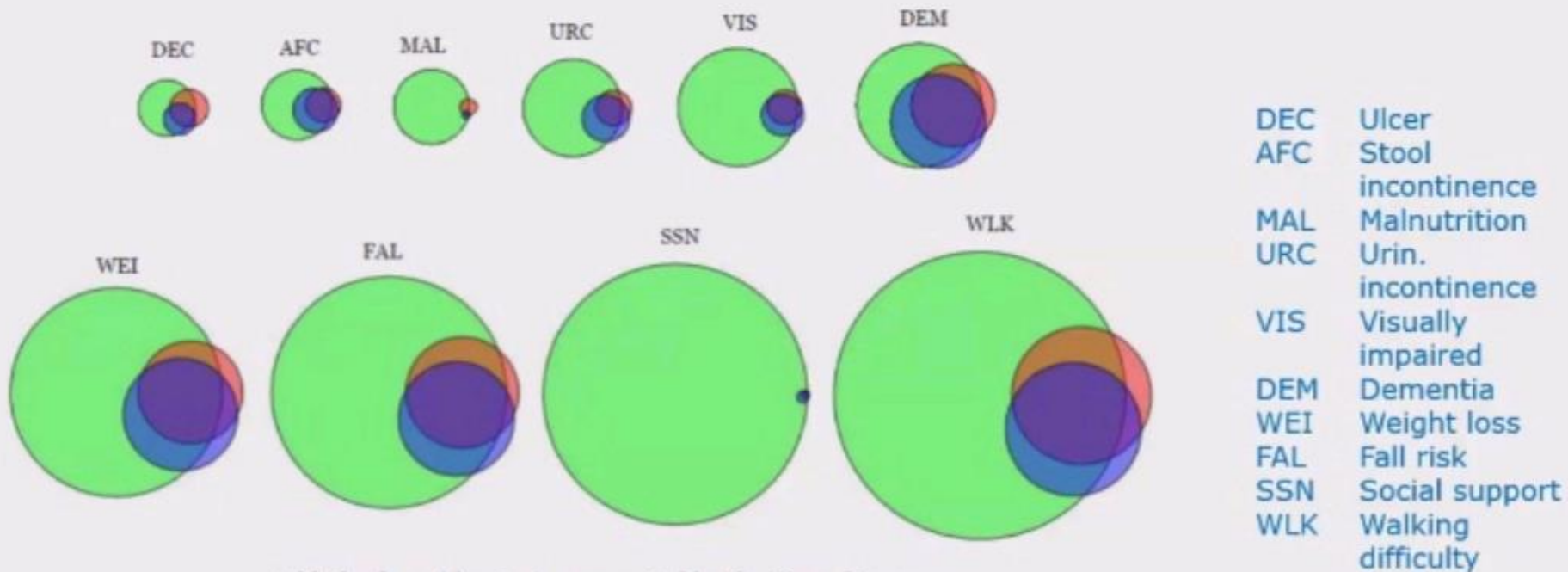
**Fig. 3 | Recommended age to start CRC screening based on a polygenic risk score.**



## Discovery of common and rare genetic risk variants for colorectal cancer

To further dissect the genetic architecture of colorectal cancer (CRC), we performed whole-genome sequencing of 1,439 cases and 720 controls, imputed discovered sequence variants and Haplotype Reference Consortium panel variants into genome-wide association study data, and tested for association in 34,869 cases and 29,051 controls. Findings were followed up in an additional 23,262 cases and 38,296 controls. We discovered a strongly protective 0.3% frequency variant signal at *CHD1*. In a combined meta-analysis of 125,478 individuals, we identified 40 new independent signals at  $P < 5 \times 10^{-8}$ , bringing the number of known independent signals for CRC to ~100. New signals implicate lower-frequency variants, Krüppel-like factors, Hedgehog signaling, Hippo-YAP signaling, long noncoding RNAs and somatic drivers, and support a role for immune function. Heritability analyses suggest that CRC risk is highly polygenic, and larger, more comprehensive studies enabling rare variant analysis will improve understanding of biology underlying this risk and influence personalized screening strategies and drug development.

# Key clinical concepts are “locked” in free text



Added value of free text represented by the Venn diagram  
 Circle sizes represent the number of patients identified by each methodology/data-source  
*Green: EHR Free Text; Blue: EHR Structured; Red: Insurance Claims*

<sup>1</sup> Source: Johns Hopkins CPHIT 2016



Convierte los datos clínicos en información accesible



- **augmentine : 0.7172036170959473**
- **azitromicina : 0.6723947525024414**
- **levofloxacino : 0.6522894501686096**
- **claritromicina : 0.6367245316505432**
- **ciprofloxacino : 0.6035829186439514**
- **penicilina : 0.5952222943305969**
- **antibiótico : 0.5926780104637146**
- **metronidazol : 0.5866072773933411**
- **ampicilina : 0.5789191126823425**
- **gentamicina : 0.5435304045677185**

Frase: No RAM conocidas [No RAM conocidas]

chunk: "No RAM conocidas"

No RAM conocidas 62014003 Reacción adversa medicamentosa (negadol) No Reacción adversa medicamentosa conocidas Score:0.9339

Frase: HTA y DLP en tratamiento

HTA 38341003 hipertensión arterial Hipertensión arterial Score:0.9890

DLP 370992007 dislipidemia Dislipidemia Score:0.9890

Frase: No DM

DM 73211009 diabetes mellitus (negadol) Diabetes mellitus Score:0.9990

Frase: cardiopatía isquémica crónica [cardiopatía isquémica crónica]

chunk: "cardiopatía isquémica crónica"

cardiopatía isquémica crónica 41383009 cardiopatía isquémica crónica cardiopatía isquémica crónica Score:0.9890

## Savana: Re-using Electronic Health Records with Artificial Intelligence

Ignacio Hernández Medrano<sup>1</sup>, Jorge Tello Guijarro<sup>1</sup>, Cristóbal Belda<sup>2</sup>, Alberto Ureña<sup>1</sup>, Ignacio Salcedo<sup>1</sup>, Luis Espinosa-Anke<sup>1,3</sup>, Horacio Saggion<sup>3</sup>

<sup>1</sup>Savana

<sup>2</sup>HM Hospital

<sup>3</sup>TALN DTIC, Universitat Pompeu Fabra, Barcelona (Spain)





demo2

## Informe 190

id: demo\_record1

Informes: 3 Evaluados: 0

SIGUIENTE INFORME

### Evolución:

79 años

paciente que estuvo ingresado en nuestro servicio marzo de 2015 por anuria obstructiva

Buen estado general. Come bien

PSA TOTAL 300,09 ng/mL

CREATININA 1,06 mg/dL

FILTRADO GLOMERULAR (CKD-EPI) 66 mL/min

Este valor es una situación frecuente en personas mayores. No indica ERC sin presencia de lesión renal (albuminuria o proteinuria elevada)

COLESTEROL TOTAL 205 mg/dL

TRIGLICERIDOS 64 mg/dL

Normal: <150

Límite alto: 150-199

Altos: >199

ALT/GPT 83 U/L

2015-06-15)

RASTREO OSEO

Texto: DATOS CLÍNICOS: Control por PSA > 500 en neo próstata. PROCEDIMIENTO: Gammagrafía ósea de cuerpo completo tras la inyección de 20 mCi de 99mTc-HDP

2015-06-17)

TC TORACO-ABDOMINO-PÉLVICO, CON CONTRASTE

Texto: INFORMACIÓN CLÍNICA - PSA > 500. TÉCNICA - se realiza TC TORACO-ABDÓMINO-PÉLVICA con adquisición helicoidal tras administración de contraste yodado

### ¿Según el informe, el paciente ha tenido / tiene cáncer de próstata?

Sí  No



#### Caracterización

Indique si aparece en el informe el valor total para la escala gleason

Sí  No

Indique si aparece en el informe, el último dato de PSA

Sí  No

Valor

300

Indique si aparece en el informe el valor T de la clasificación TNM

Sí  No

Indique si aparece en el informe el valor N de la clasificación TNM

Sí  No

Indique si aparece en el informe el valor M de la clasificación TNM

Sí  No

Diagnóstico

Tratamiento

## Validación de Savana en cardiopatía isquémica, por cardiólogos

### Hospital 1

Primary variable	TP	FP	FN	Precision	Recall	F-score
Hipercolesterolemia primaria	9	0	0	1,00	1,00	1,00
Hipertrigliceridemia	6	0	0	1,00	1,00	1,00
Infarto agudo de miocardio	5	0	0	1,00	1,00	1,00
Angina estable	1	2	0	0,33	1,00	0,50
Cardiopatía isquémica	26	5	0	0,84	1,00	0,91
Accidente cerebrovascular (ACVA), Ictus	5	6	10	0,45	0,33	0,38
Accidente isquémico transitorio (AIT, TIA)	4	0	0	1,00	1,00	1,00
Diabetes mellitus	157	0	3	1,00	0,98	0,99
Enfermedad renal crónica	36	0	10	1,00	0,78	0,88
Aterosclerosis carotídea	0	0	4	0,00	0,00	0,00
Enfermedad coronaria multivaso	0	4	0	0,00	0,00	0,00
Enfermedad coronaria de 1 vaso	0	0	4	0,00	0,00	0,00

0,96

### Hospital 2

Primary variable	TP	FP	FN	Precision	Recall	F-score
Síndrome coronario agudo	1	0	0	1,00	1,00	1,00
Angina estable	1	1	0	0,50	1,00	0,67
Cardiopatía isquémica	9	0	0	1,00	1,00	1,00
Accidente cerebrovascular (ACVA), Ictus	8	0	0	1,00	1,00	1,00
Enfermedad arterial periférica	1	0	0	1,00	1,00	1,00
Diabetes mellitus	30	0	2	1,00	0,94	0,97
Enfermedad renal crónica	3	0	2	1,00	0,60	0,75



El Servicio de Salud de Castilla-La Mancha (SESCAM) es la institución encargada de la gestión de la salud en la comunidad autónoma de Castilla-La Mancha.

### Objetivo del proyecto

Implantar un sistema de soporte a la decisión en tiempo real que mejorase la adherencia de los profesionales del SESCAM a las diferentes vías clínicas establecidas por dicho Servicio de Salud.

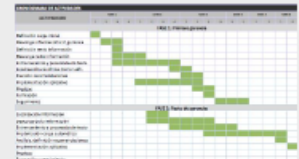
### La importancia de la adherencia a las vías clínicas

La vía clínica es una herramienta organizativa multidisciplinaria que permite llevar a cabo una secuencia óptima para llegar a un determinado diagnóstico o realizar un procedimiento, donde se incluyen todas las diferentes actividades de los profesionales que intervienen en la atención al paciente durante la estancia hospitalaria o cuando acude a consulta. Las vías clínicas son una de las principales herramientas de la gestión de la calidad asistencial para la estandarización de los procesos asistenciales y su implantación permite disminuir la variabilidad de la práctica clínica.

### 3 fases de proyecto

1. Utilizando la tecnología de **SAVANA Manager** se ha analizado toda información clínica necesaria para poder cuantificar la adherencia a las distintas vías y se han establecido recomendaciones que ayuden a mejorar los índices de adherencia.
2. Se ha habilitado en cada estación clínica objetivo el sistema de soporte en tiempo real desarrollado por **Accenture** con la tecnología de **Procesado del Leng** Primaria cuando al proceso asistencial prueba se ha implantado en 5 meses, en el Área de Atención Primaria de Mancha Centro.
3. Se ha monitorizado

de las mejores prácticas.



### Resultados

- La adherencia a las vías clínicas ha mejorado en 8 vías clínicas, siendo significativo ( $p < 0,05$ ) en 3 de ellas.
- Los usuarios de los Centros de Salud ven la solución como un instrumento útil que no entorpece ni afecta a la dinámica de su trabajo.

"La tecnología de Savana es flexible y maneja diferentes tipos de formato, siempre que sean de tipo texto. El uso de herramientas avanzadas de análisis de datos y servicios terminológicos permiten extraer de los sistemas una información de valor para el clínico. Dispone de un algoritmo de anonimización que cumple con todos los requerimientos de privacidad.

"La implantación de la solución de Savana/Accenture ha supuesto una mejora en la adherencia a las vías clínicas, lo que ha repercutido muy positivamente en la calidad asistencial, y ayudando al profesional en la toma de decisiones y disminuyendo la variabilidad de la práctica clínica en nuestros centros"

*Este documento ha sido descargado de la web del Club Excelencia en Gestión: [www.clubexcelencia.org](http://www.clubexcelencia.org)*

**Dr. Luis Morell Baladrón**

Director de Sistemas de la Información SESCAM

**Dr. Alfonso Abaigar**

Director de Atención Primaria SESCAM



# Hiperpotasemias en un click con Savana

P. DE SEQUERA, P. ARRANZ\*, M. ALBALATE, E. CORCHETE, R. PÉREZ-GARCÍA, M. ORTEGA-GÓMEZ, M. PUERTA, R. ALCÁZAR, C. RUIZ-CARO, J. MARTÍN-NAVARRO. S. Nefrología. S. de Control de Gestión. Hospital Universitario Infanta Leonor.



## INTRODUCCIÓN

La hiperpotasemia, definida como una concentración de potasio en plasma mayor de 5 mmol/L, es un trastorno electrolítico grave, que se asocia con mayor mortalidad, y cuya incidencia está aumentando.



## OBJETIVO

Estudiar la epidemiología de la hiperpotasemia en nuestro hospital investigando a través del S. Admisión-Documentación clínica y con el buscador SAVANA.

## MÉTODOS

Estudio transversal y observacional durante un año (01/01/2016-31/12/2016), que incluye a adultos mayores de 18 años con el diagnóstico principal o secundario en el informe de alta de hiperpotasemia, con los datos

XXXIX Congreso SEME / VI Congreso Ibérico / XXXVI Congreso SOCALME

V. 37

### ENCEFALOPATÍA DE WERNICKE. ESTUDIO RETROSPECTIVO 2011-2016 MEDIANTE SISTEMA DE BÚSQUEDA SAVANA

M. Ulla Azeitegui<sup>1</sup>, B. Escobedo<sup>1</sup>, T. Balderas<sup>1</sup>, R. Pacheco<sup>1</sup>, G. P. Meléndez<sup>1</sup>, V. Parde<sup>1</sup>, M. Duffel<sup>1</sup> <sup>1</sup>M. Interna. Hospital Infanta Leonor. Madrid (Madrid)

#### OBJETIVOS

La Encefalopatía de Wernicke (EW) es una entidad infrecuentemente diagnosticada que se asocia habitualmente a alcoholismo. Se caracteriza por la tríada clásica (encefalopatía, oftalmoplejía y ataxia). En series de seguimiento, la EW fue diagnosticada en vida sólo en un tercio de los pacientes. Nuestro trabajo es un estudio descriptivo de los pacientes con EW ingresados en el Hospital Universitario Infanta Leonor durante el periodo 2011-2016, utilizando la herramienta de búsqueda SAVANA, de reciente implementación en nuestro hospital.

#### MATERIAL Y MÉTODOS

Estudio transversal y observacional, periodo Enero-2011 a Diciembre 2016, que incluye a adultos con diagnóstico principal o secundario en el informe de alta de EW. El sistema SAVANA es una plataforma de búsqueda con capacidad de reutilizar el contenido de las historias clínicas electrónicas, directamente desde la información no estructurada (escrita en lenguaje natural o texto libre). Tiene capacidad para realizar en un "click" una búsqueda en los 3,5 millones de documentos del hospital.

#### RESULTADOS

36 episodios de ingreso en 24 pacientes. 58%V, 42%M. Edad X 51a. Desviación típica 9a, Moda 48a. Servicios implicados en el manejo: Neurología 47%, M. Interno 19%, Uroginecología 19%, A.Digestivo 8%, Cirugía General/Digestiva 3%, Unidad Hospitalización Media Estancia 3%. Antecedentes Personales: Alcoholismo 50% (Edad X 54a, V 66,6%), Delirium 16% (Edad X 58a, V 100%), Deterioro Cognitivo/Demencia 16% (Edad X 60a, V100%), Cirrosis Hepática 11% (Edad X 60a, V 100%). Varios Eosinofílicos 8% (Edad X 60a, V 100%). Pruebas Complementarias durante el ingreso: TAC 39% de los pacientes (49% normal), RMN 17% (80% normal), Serologías Víricas (hepatovirus, VHB) 25%, Estudio Hormonal (función tiroidea y suprarrenal) 11%, Estudio Endoscópico Alto 11%. Tratamiento durante el ingreso: Inhibidores de la Bomba de Protones 61%, Vasopresina B (Tiamina 28%, Piridoxina 22%, complejo B1-B6-B12 17%, B12 y Ácido Fólico 22%), Antipsicóticos (Tioridol) 39%, Lactulosa 39%, Ansiolíticos ( Clonazepam Diposolón) 33%, Paracetamol 22%, Espironolactona 22%, Antidopaminérgicos (Venlafaxina)17%, (tramadol) 17%.

#### DISCUSIÓN

En nuestro estudio, más del 80% de los casos de EW se relacionan con malnutrición asociada al abuso de alcohol. No obstante, procesos reopáticos, cirugía gastrointestinal, hipertiroidismo y apandicitomía pueden desencadenar una EW sin antecedentes previos de etilismo. El tratamiento es sencillo (reposición intravenosa de Tiamina durante 3-5 días). No obstante, dosis subterapéuticas o la ausencia de tratamiento pueden ocasionar la muerte (20% de los casos) o un Síndrome de Korsakoff (forma irreversible de amnesia atencional). En nuestra serie, la prevalencia de EW en el sexo femenino es elevada (42%), aunque su asociación con procesos como la hepatopatía alcohólica (cirrosis) ocurre de forma privativa en los varones. No es infrecuente el desarrollo de Síndrome Confusional (en relación con deprivación alcohólica). En la mitad de los pacientes, precisa de pruebas de imagen cerebral (TAC,RMN) para descartar otra etiología. La administración de Tiamina (sólo o asociada a B6-B12) se objetiva en el 45% de los casos, en el resto, el diagnóstico de EW probablemente se efectuó en proceso previo (36 episodios en 24 pacientes).

#### CONCLUSIONES

1.- En nuestra serie, hay alta prevalencia de EW en mujeres (en la bibliografía 2-3 veces más prevalente en el sexo masculino). 2.-La relación EW y alcohol es indiscutible, acompañándose en ocasiones de Síndrome Confusional. Agudo en el contexto de deprivación alcohólica. 3.- Se ha administrado Tiamina en la mitad de los



## 7. ASTHMA EMERGENCIAS IN AN ADULT OF MADRID (SPAIN)

M. Garcimartín Galicia M.I., R. Somosa Álvarez M.L., Pérez-Alcalá M. Leonor University Hospital, Madrid

plataforma capaz de reutilizar el contenido de la información no

#### BACKGROUND:

- Asthma is a heterogeneous chronic inflammatory airways disease that represents a prevalence and increasing trends in morbidity. Each year in Western Europe emergency health care and 10% require an emergency department visit.
- The aim of this study is to describe the epidemiological features, exacerbation of patients with emergency admissions for asthma

#### MATERIAL AND METHODS:

- We conducted a retrospective descriptive study of the emergency visits for asthma Leonor University Hospital (Madrid, Spain).
- Data were collected from the electronic clinical history, using the Ehealther technology of medical concepts using controlled terminology basis and computational linguistic

#### RESULTS:

- 776 emergency admissions for asthma, in 671 patients were included
- Mean age was 53 ± 22 years, mode 50 years and 73% were female

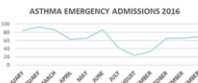


Figure 1. Asthma emergency admissions. Distribution by months

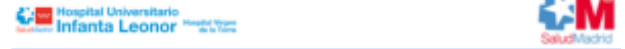
DISCHARGED TREATMENT	% PATIENTS	DIAGNOSIS TESTS	% PATIENTS
Sabutamol	80	Blood gas	41
ICS	23	Blood test	52
LABA/ICS	21	Chest X-Ray	49
LAMA	40	EKG	20
Oral corticosteroid	68	CT	3
Antibiotics	23	Flu test	5

#### CONCLUSIONS:

- The profile of a patient that requires an emergency visit due to an asthma exacerbation is a medium age female.
- Asthma exacerbations in Madrid are seasonal, in winter and spring, in relation with respiratory infections and pollen exposure respectively.

#### REFERENCES:

http://www.polenes.com/home



## CAMBIOS EPIDEMIOLÓGICOS EN LA PATOLOGÍA VALVULAR EN LOS ÚLTIMOS 10 AÑOS: IMPLICACIONES FUTURAS EN EL ABORDAJE TERAPEUTICO

Cristina de Carlos Casanova<sup>1</sup>, M<sup>a</sup> Del Mar Sancho Castañó<sup>1</sup>, Laura María Yagüe<sup>1</sup>, Silvia Jiménez Loeches<sup>1</sup>, Eloy Gómez Martínez<sup>1</sup>, Verónica Suberbiola Sánchez-Caballero<sup>1</sup>, Cristina Beltrán Harms<sup>1</sup>, David Viquezta Cabilío<sup>1</sup> y Roberto Muñoz-Agüero<sup>1</sup> <sup>1</sup>Hospital Universitario Infanta Leonor. Madrid

INTRODUCCIÓN: Hay pocos datos actualizados sobre la epidemiología de la enfermedad valvular (EV) en nuestro país. Debido a un envejecimiento y por tanto, una mayor supervivencia media de la población, la prevalencia de la EV está aumentando. Los pacientes con EV tienen una mayor comorbilidad, lo que confiere un mayor riesgo quirúrgico. El objetivo de este estudio fue describir la prevalencia y distribución temporal de la EV en el área de población de referencia de nuestro centro hospitalario a lo largo del periodo 2008-2017 y describir las principales características demográficas de los pacientes con EV, comparándolos con los de la población del EuroHeartSurvey.

MÉTODOS: Mediante el empleo de una nueva herramienta tecnológica (Savana®) basada en la tecnología EHRdata, diseñada para el análisis del big data en términos descriptivos y predictivos, se extrajo la información clínica relevante de las historias médicas electrónicas. Se analizaron todos los informes generados en el área de hospitalización, urgencias o consultas externas de nuestro hospital. Fueron seleccionados los pacientes con un diagnóstico de EV moderada o severa. Se estimó la prevalencia de EV en 2 periodos de tiempo, desde Febrero 2009 hasta Febrero 2013 y desde Marzo 2013 hasta Diciembre 2017.

RESULTADOS: La prevalencia de EV en nuestra población fue 1,04% (n=5431). La insuficiencia mitral fue la valvulopatía más frecuente (5,4%, n=1318), seguida de la estenosis aórtica (5,3%, n=967) e insuficiencia aórtica (2,2%, n=930). Hubo una clara predominancia del sexo femenino (52%, Figura 1), y la edad media fue 70 años (edad media EuroHeartSurvey 65 años, Figura 1). En el primer periodo (2009-2013) la prevalencia fue 0,25%, con un aumento significativo hasta 0,70% en el segundo periodo (2013-2018). Esta tendencia fue consistente en todos los tipos de valvulopatías (Figura 2). La prevalencia de las distintas comorbilidades fue mayor que en otros estudios epidemiológicos previamente publicados (Tabla 1).

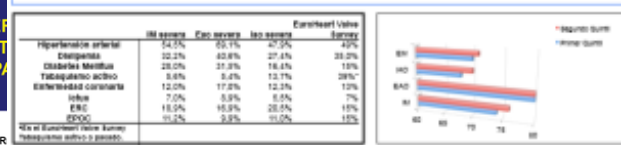


Tabla 1. Comparación de las prevalencias de valvulopatías entre la población de nuestro centro hospitalario con el EuroHeart Survey. Figura 1. Edad media de los diferentes tipos de valvulopatías en el primer y segundo quinquenio

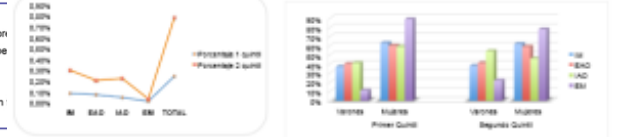


Figura 2. Distribución de las prevalencias de las valvulopatías en el primer y segundo quinquenio

CONCLUSIÓN: En nuestra serie en los últimos 10 años, hay un claro aumento en la edad de presentación de la enfermedad valvular moderada/severa y con un gran número de comorbilidades comparado con el EuroHeart Survey, lo que refuerza la idea de que las nuevas terapias percutáneas deberán jugar un papel fundamental en el tratamiento de este tipo de pacientes. Aunque la prevalencia puede estar inflacionada en nuestra población, debido a la metodología, refleja una patología en aumento diagnosticada en pacientes de edad más avanzada y cada vez más enfermos.



Figure 2. Pollen levels in Madrid (Spain) in 2016

41% exacerbations triggered by respiratory infections

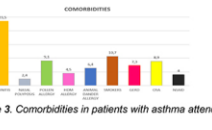
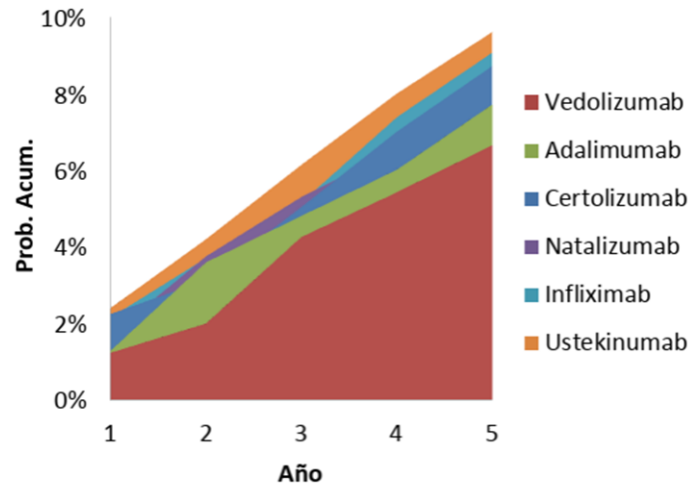
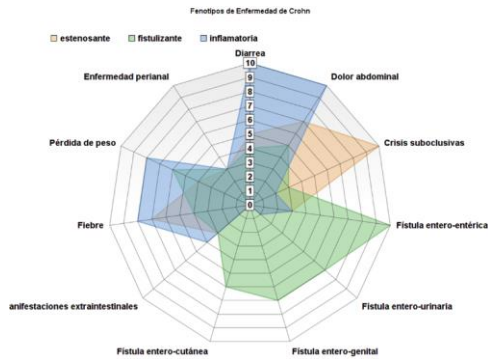
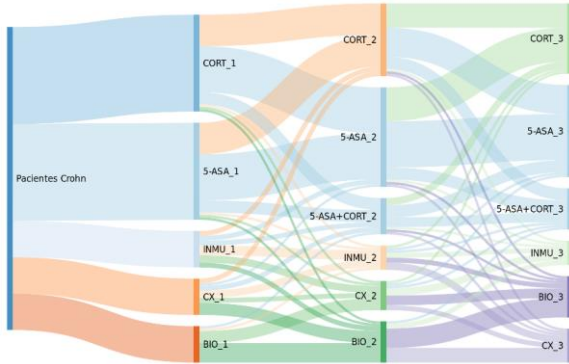


Figure 3. Comorbidities in patients with asthma attendance

# ENFERMEDAD INFLAMATORIA:

patient journey, predicción de respuesta a biológicos, fenotipado automático



Proyecto seleccionado por la  
Comisión Europea



10

ENTRE

2500

EMPRESAS  
TECNOLÓGICAS



France

Belgium

Austria

España

Switzerland

United Kingdom

Ireland

Germany



SAVANA

SavanaManager

## Predictive Patient Surveillance System Receives FDA Clearance

Ryan Black  
JANUARY 08, 2018



(WAVE Clinical Platform. Image courtesy Excel Medical.)

Florida-based medical device maker Excel Medical today announced that its WAVE Clinical Platform has received clearance from the FDA. The system allows for constant patient monitoring, analyzed and delivered to hospital staff in real time, to prevent unexpected deaths in the hospital.

PubMed Evidence-Based Pediatric Outcom  
US National Library of Medicine  
National Institutes of Health  
Advanced

Format: Abstract ▾

*Pediatr Crit Care Med.* 2015 Sep;16(7):e207-16. doi: 10.1097/PCC.0000000000000481.

## Evidence-Based Pediatric Outcome Predictors to Guide the Allocation of Critical Care Resources in a Mass Casualty Event.

Toltzis P<sup>1</sup>, Soto-Campos G, Shelton C, Kuhn EM, Hahn R, Ka

biomedical engineering ARTICLES

PLOS ONE

RESEARCH ARTICLE

### Personalized survival predictions via Trees of Predictors: An application to cardiac transplantation

Jinsung Yoon<sup>1</sup>, William R. Zame<sup>1</sup>, Amitava Banerjee<sup>2</sup>, Martin Cadeiras<sup>3</sup>, Ahmed M. Alaa<sup>4</sup>, Mihaela van der Schaar<sup>1,3,4\*</sup>

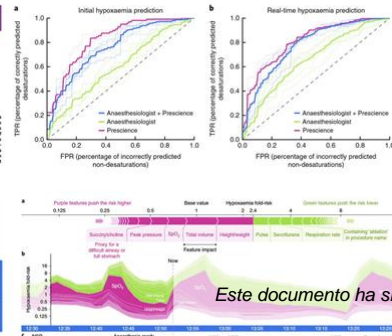
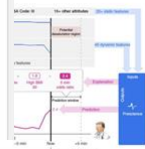
<sup>1</sup> University of California Los Angeles, Los Angeles, California, United States of America, <sup>2</sup> Fair Institute of Health Informatics Research, University College, London, United Kingdom, <sup>3</sup> University of Oxford, Oxford, United Kingdom, <sup>4</sup> Alan Turing Institute, London, United Kingdom

\* mihaela.vanderschaar@oxford-man.ox.ac.uk

### Machine learning predictions for hypoxemia during surgery

Yoon<sup>1</sup>, Maynard-Harber<sup>1</sup>, Michael J. Eissa<sup>1\*</sup>, van<sup>1</sup>, Soto-Campos<sup>1</sup>, Jerry Kim<sup>1</sup> and

Machine learning predictions for hypoxemia during surgery. This study aims to predict hypoxemia during surgery using machine learning. The study involves collecting data from patients during surgery and using machine learning algorithms to predict hypoxemia. The results show that machine learning can accurately predict hypoxemia during surgery.



Resources How To  
PMC  
Library of Medicine  
National Institutes of Health  
Advanced Journal list  
List > HHS Author Manuscripts > PMC3673290

HHS Public Access  
Author manuscript  
Peer-reviewed and accepted for publication  
About author manuscripts Submit a manuscript

*Crit Care Med.* Author manuscript; available in PMC 2013 Jun 5.  
Published in final edited form as:  
*Crit Care Med.* 2011 Jan; 39(1): 65–72.  
doi: 10.1097/CCM.0b013e3181fb7b1c

PMCID:  
NIHMSID: 1

## Cardiorespiratory integrated monitoring

Marilyn Hravnak, PhD, Michael A. D

JAMA Surgery Journals Enter Search Term  
The Value of Clinical Colorectal Cancer Registries in Colorectal Cancer Research  
Review | June 20, 2018

New Online Views 0 Citations 0 Altmetric 14

Surgical Innovation

June 20, 2018

## Automated Performance Metrics and Machine Learning Algorithms to Measure Surgeon Performance and Anticipate Clinical Outcomes in Robotic Surgery

Andrew J. Hung, MD<sup>1</sup>, Jian Chen, MD<sup>2</sup>, Inderbir S. Gill, MD<sup>3</sup>

Author Affiliations

ScienceRobotics Home News Journals Topics Careers  
Search jobs on ScienceCareers.org  
Science Careers FROM THE JOURNAL SCIENCE  
Log In | My  
SHARE RESEARCH ARTICLE HUMAN-ROBOT INTERACTION  
Personalized machine learning for robot perception of affect and engagement in autism therapy  
Ognjen Rudovic<sup>1\*</sup>, Jaeryoung Lee<sup>2</sup>, Miles Dai<sup>1</sup>, Björn Schuller<sup>3,4</sup> and Rosalind W. Picard<sup>1</sup>  
See all authors and affiliations  
Science Robotics 27 Jun 2018:  
Vol. 3, Issue 19, eaa6760  
DOI: 10.1126/scirobotics.aag6760

## Real-time localization of surgically resectable lesions in a multi-analyte blood test

Li<sup>1</sup>, Yuxuan Wang<sup>1,2,3,4</sup>, Christopher Thoburn<sup>1</sup>, Bahman Afsari<sup>1</sup>, Ludmila Danilova<sup>1</sup>, Christopher ...

DOI: 10.1126/science.aar3247

Send to ▾

Article Figures & Data Info & Metrics eLetters PDF

You are currently viewing the abstract.

View Full Text ▶

### Abstract

Earlier detection is key to reducing cancer deaths. Here we describe a blood test that can detect eight common cancer types through assessment of the levels of circulating proteins and mutations in cell-free DNA. We applied this test, called CancerSEEK, to 1,005 patients with non-metastatic colorectal cancer (ovary, liver, stomach, bladder, and pancreatic cancer).

npj Digital Medicine

Article | OPEN | Published: 06 November 2018

## Machine-learned epidemiology: real-time detection of foodborne illness at scale

Adam Sadilek, Stephanie Caty, Lauren DiPrete, Raed Mansour, Tom Schenk Jr, Mark Bergtholdt, Ashish Jha, Prem Kamaswami & Evgeny Gaidarov

npj Digital Medicine 1, Article number: 36 (2018) | Download Citation ↓

Este documento ha sido descargado de la web del Club Excelencia en Gestión: www.clubexcelencia.org

**Table 1 | Peer-reviewed publications of AI algorithms compared with doctors**

Specialty	Images	Publication	
Radiology/neurology	CT head, acute neurological events	Nam et al. <sup>8</sup>	
	CT head for brain hemorrhage	Arbabshirani et al. <sup>19</sup>	
	CT head for trauma	Chilamkurthy et al. <sup>20</sup>	
	CXR for metastatic lung nodules	Nam et al. <sup>8</sup>	
	CXR for multiple findings	Singh et al. <sup>7</sup>	
	Mammography for breast density*	Lehman et al. <sup>26</sup>	
Pathology	Wrist X-ray	Lindsey et al. <sup>9</sup>	
	Breast cancer	Bejnordi et al. <sup>3</sup>	
	Lung cancer (+ driver mutation)	Coudray et al. <sup>33</sup>	
	Brain tumors (+ methylation)	Capper et al. <sup>45</sup>	
	Breast cancer metastases*	Steiner et al. <sup>35</sup>	
Dermatology	Breast cancer metastases	Liu et al. <sup>34</sup>	
	Skin cancers	Esteva et al. <sup>47</sup>	
	Melanoma	Haenssle et al. <sup>48</sup>	
	Skin lesions	Han et al. <sup>49</sup>	
Ophthalmology	Diabetic retinopathy	Gulshan et al. <sup>51</sup>	
	Diabetic retinopathy*	Abramoff et al. <sup>31</sup>	
	Diabetic retinopathy*	Kanagasigam et al. <sup>32</sup>	
	Congenital cataracts	Long et al. <sup>38</sup>	
	Retinal diseases (OCT)	De Fauw et al. <sup>56</sup>	
	Macular degeneration	Burlina et al. <sup>52</sup>	
	Retinopathy of prematurity	Brown et al. <sup>60</sup>	
	AMD and diabetic retinopathy	Kermary et al.	
	Gastroenterology	Polyyps at colonoscopy*	Mori et al.
		Polyyps at colonoscopy	Wang et al. <sup>37</sup>
Cardiology	Echocardiography	Madani et al.	
	Echocardiography	Zhang et al. <sup>24</sup>	

**Table 3 | Selected reports of machine- and deep-learning algorithms to predict clinical outcomes and related parameters**

Prediction	n	AUC	Publication (Reference number)
In-hospital mortality, unplanned readmission, prolonged LOS, final discharge diagnosis	216,221	0.93*0.75+0.85#	Rajkomar et al. <sup>96</sup>
All-cause 3-12 month mortality	221,284	0.93 <sup>†</sup>	Avati et al. <sup>91</sup>
Readmission	1,068	0.78	Shameer et al. <sup>106</sup>
Sepsis	230,936	0.67	Horng et al. <sup>102</sup>
Septic shock	16,234	0.83	Henry et al. <sup>103</sup>
Severe sepsis	203,000	0.85 <sup>@</sup>	Culliton et al. <sup>104</sup>
<i>Clostridium difficile</i> infection	256,732	0.82 <sup>++</sup>	Oh et al. <sup>93</sup>
Developing diseases	704,587	range	Miotto et al. <sup>97</sup>
Diagnosis	18,590	0.96	Yang et al. <sup>90</sup>
Dementia	76,367	0.91	Cleret de Langavant et al. <sup>92</sup>
Alzheimer's Disease (+ amyloid imaging)	273	0.91	Mathotaarachchi et al. <sup>98</sup>
Mortality after cancer chemotherapy	26,946	0.94	Elfiky et al. <sup>95</sup>
Disease onset for 133 conditions	298,000	range	Razavian et al. <sup>105</sup>
Suicide	5,543	0.84	Walsh et al. <sup>86</sup>
Delirium	18,223	0.68	Wong et al. <sup>100</sup>



INCLUDE FEATURES

EXCLUDE FEATURES

Have you considered these? [Hide](#)Recurrent Staphylococcus aureus infections [+](#)

Discoid lupus rash

Decreased activity of NADPH oxidase

Your Patient Profile [Remove all](#) Eczematoid dermatitis [Onset](#) Thrombocytopenia [Onset](#)

Any known affected family member?

[ADD A RELATIVE](#)**GENE RESULTS:** SLC02A1, HPGD, WAS, WIPF1, LBR, HLCS, PCCB, PCCA, STAT1, SBDS, RBM8A, FLI1, NSUN2, LIG4

DISEASES

PANELS

11 Results

**PACHYDERMOPERIOSTOSIS**[Dismiss](#)

SLC02A1, HPGD

Primary hypertrophic osteoarthropathy is a familial disorder characterized by digital clubbing and osteoarthropathy, wit...

**Clinical Features**[See More Clinical Features](#)

Hepatomegaly

Large fontanelles

Arthropathy

**PELGER-HUET ANOMALY**[Dismiss](#)

LBR

This disease is listed on OMIM  
[Click here for more information](#)**PROPIONIC ACIDEMIA**[Dismiss](#)

PCCB, PCCA

Also known as: Propionyl-coa carboxylase deficiency; Pcc deficiency; Glycinemia, ketotic; Hyperglycinemia with ketoacidosis and leukope...

**SHWACHMAN-DIAMOND SYNDROME**[Dismiss](#)

SBDS

Shwachman-Diamond syndrome is a multisystem autosomal recessive disorder characterized by exocrine pancreatic dysfunctio...

**JACOBSEN SYNDROME**[Dismiss](#)

FLI1

Also known as: Chromosome 11q deletion syndrome; Partial 11q monosomy syndrome...

**WISKOTT-ALDRICH SYNDROME**[Dismiss](#)

WAS, WIPF1

Wiskott-Aldrich syndrome is an X-linked recessive immunodeficiency characterized by thrombocytopenia, eczema, and recurr...

**Clinical Features**[See More Clinical Features](#)

Specific learning disability

Abnormality of eosinophils

Blepharitis

**HOLOCARBOXYLASE SYNTHETASE DEFICIENCY**[Dismiss](#)

HLCS

Holocarboxylase synthetase deficiency, a biotin-responsive multiple carboxylase deficiency (MCD), is characterized by me...

**IMMUNODEFICIENCY 31C**[Dismiss](#)

STAT1

Immunodeficiency-31C is an autosomal dominant disorder of immunologic dysregulation with highly variable manifestations...

**THROMBOCYTOPENIA-ABSENT RADIUS SYNDROME**[Dismiss](#)

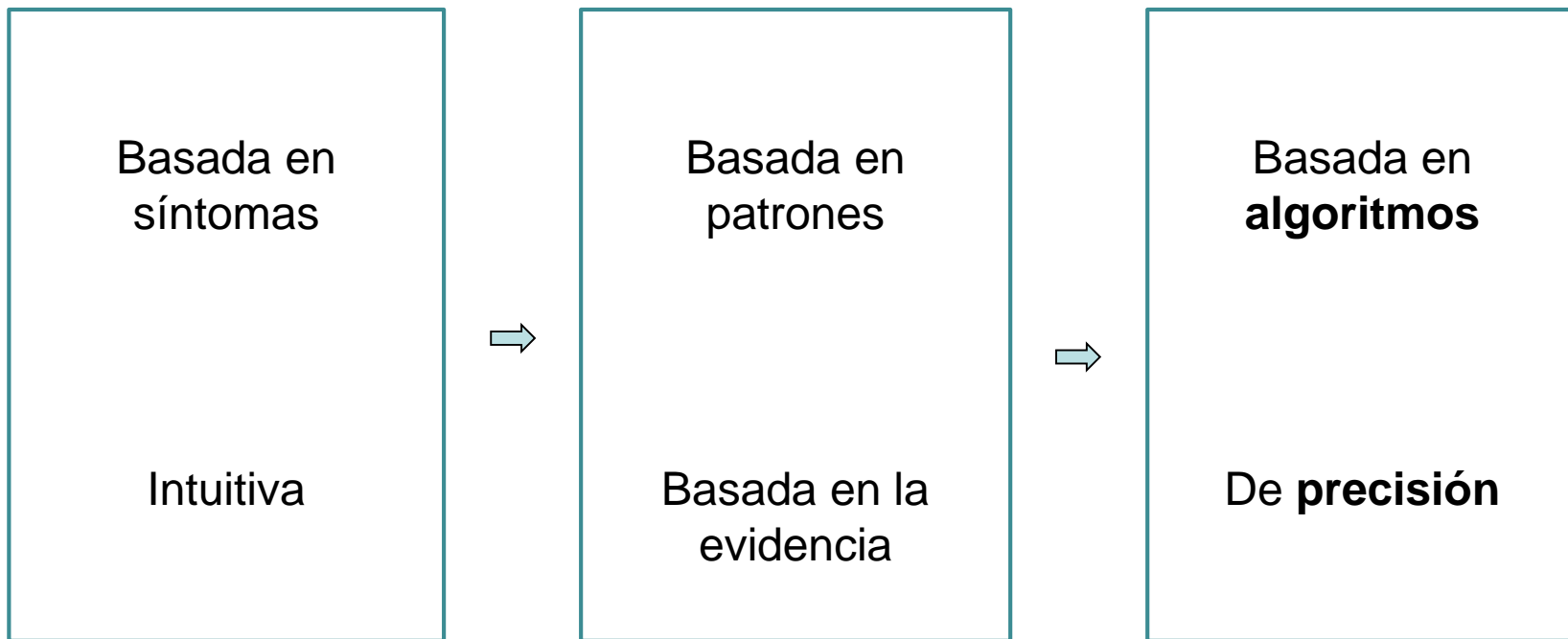
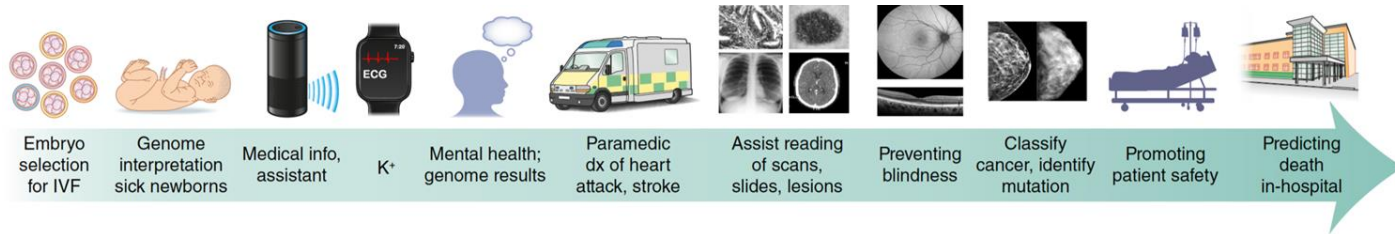
RBM8A

The thrombocytopenia-absent radius syndrome (TAR) is characterized by reduction in the number of platelets and absence o...

**DUBOWITZ SYNDROME**[Dismiss](#)

NSUN2, LIG4

This disease is listed on ORPHANET and OMIM  
[Click here for more information](#)





nature  
medicine

LETTERS

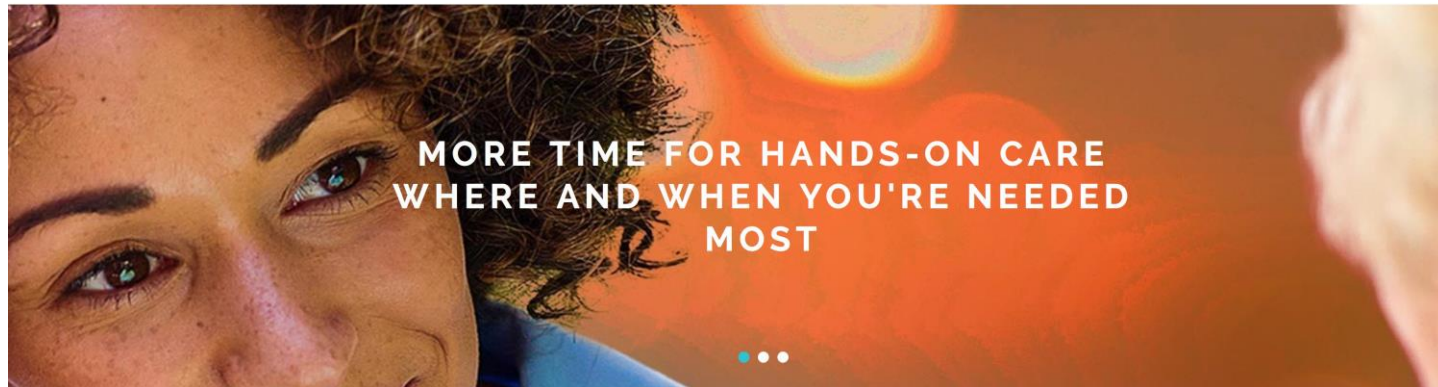
<https://doi.org/10.1038/s41591-018-0335-9>

## Evaluation and accurate diagnoses of pediatric diseases using artificial intelligence

Huiying Liang<sup>1,2</sup>, Brian Y. Tsui<sup>2,7</sup>, Hao Ni<sup>1,2,7</sup>, Carolina C. S. Valentim<sup>2,7</sup>, Sally L. Baxter<sup>2,7</sup>, Guangjian Liu<sup>1</sup>, Wenjia Cai<sup>2</sup>, Daniel S. Kermany<sup>1,2</sup>, Xin Sun<sup>1</sup>, Jiancong Chen<sup>2</sup>, Liya He<sup>1</sup>, Jie Zhu<sup>1</sup>, Pin Tian<sup>2</sup>, Hua Shao<sup>2</sup>, Lianghong Zheng<sup>4,5</sup>, Rui Hou<sup>4,5</sup>, Sierra Hewett<sup>1,2</sup>, Gen Li<sup>1,2</sup>, Ping Liang<sup>3</sup>, Xuan Zang<sup>3</sup>, Zhiqi Zhang<sup>3</sup>, Liyan Pan<sup>1</sup>, Huimin Cai<sup>4,5</sup>, Rujuan Ling<sup>1</sup>, Shuhua Li<sup>1</sup>, Yongwang Cui<sup>1</sup>, Shusheng Tang<sup>1</sup>, Hong Ye<sup>1</sup>, Xiaoyan Huang<sup>1</sup>, Waner He<sup>1</sup>, Wenqing Liang<sup>1</sup>, Qing Zhang<sup>1</sup>, Jianmin Jiang<sup>1</sup>, Wei Yu<sup>1</sup>, Jianqun Gao<sup>1</sup>, Wanxing Ou<sup>1</sup>, Yingmin Deng<sup>1</sup>, Qiaozhen Hou<sup>1</sup>, Bei Wang<sup>1</sup>, Cuichan Yao<sup>1</sup>, Yan Liang<sup>1</sup>, Shu Zhang<sup>1</sup>, Yaou Duan<sup>2</sup>, Runze Zhang<sup>2</sup>, Sarah Gibson<sup>2</sup>, Charlotte L. Zhang<sup>2</sup>, Oulan Li<sup>2</sup>, Edward D. Zhang<sup>2</sup>, Gabriel Karin<sup>2</sup>, Nathan Nguyen<sup>2</sup>, Xiaokang Wu<sup>1,2</sup>, Cindy Wen<sup>2</sup>, Jie Xu<sup>2</sup>, Wenqin Xu<sup>2</sup>, Bochu Wang<sup>2</sup>, Winston Wang<sup>2</sup>, Jing Li<sup>1,2</sup>, Bianca Pizzato<sup>2</sup>, Caroline Bao<sup>2</sup>, Daoman Xiang<sup>1</sup>, Wanting He<sup>1,2</sup>, Suiqin He<sup>2</sup>, Yugui Zhou<sup>1,2</sup>, Weldon Haw<sup>2,6</sup>, Michael Goldbaum<sup>2</sup>, Adriana Tremoulet<sup>2</sup>, Chun-Nan Hsu<sup>2</sup>, Hannah Carter<sup>2</sup>, Long Zhu<sup>3</sup>, Kang Zhang<sup>1,2,6\*</sup> and Huimin Xia<sup>2\*</sup>



100.000 cabinas x 100 pacientes/día



## When AIs Outperform Doctors: The Dangers of a Tort-Induced Over-Reliance on Machine Learning and What (Not) to Do About it

*[University of Miami Legal Studies Research Paper No. 18-3](#)*

57 Pages • Posted: 13 Feb 2018

[A. Michael Froomkin](#)

University of Miami - School of Law

[Ian R. Kerr](#)

University of Ottawa - Common Law Section

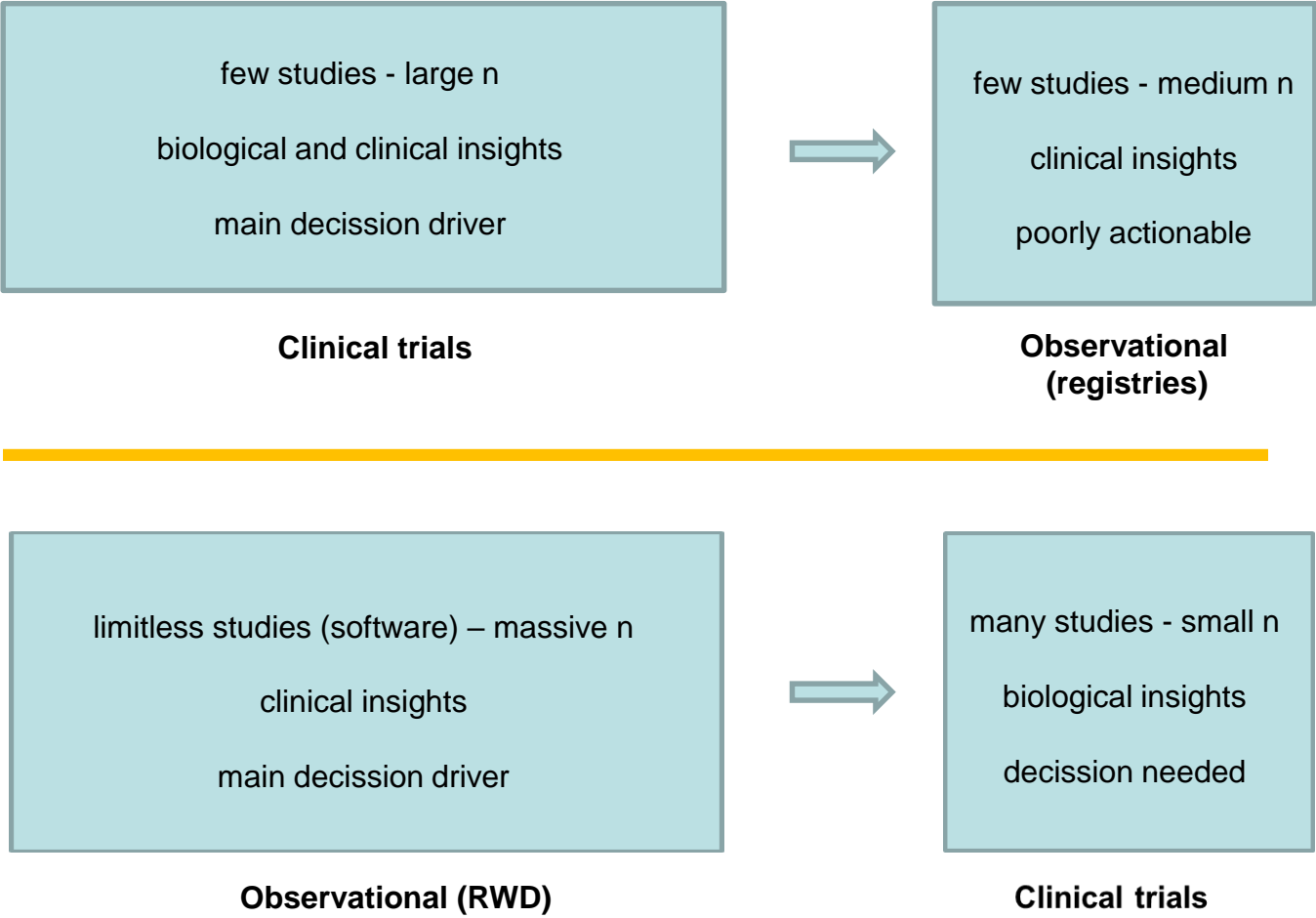
[Joelle Pineau](#)

McGill University

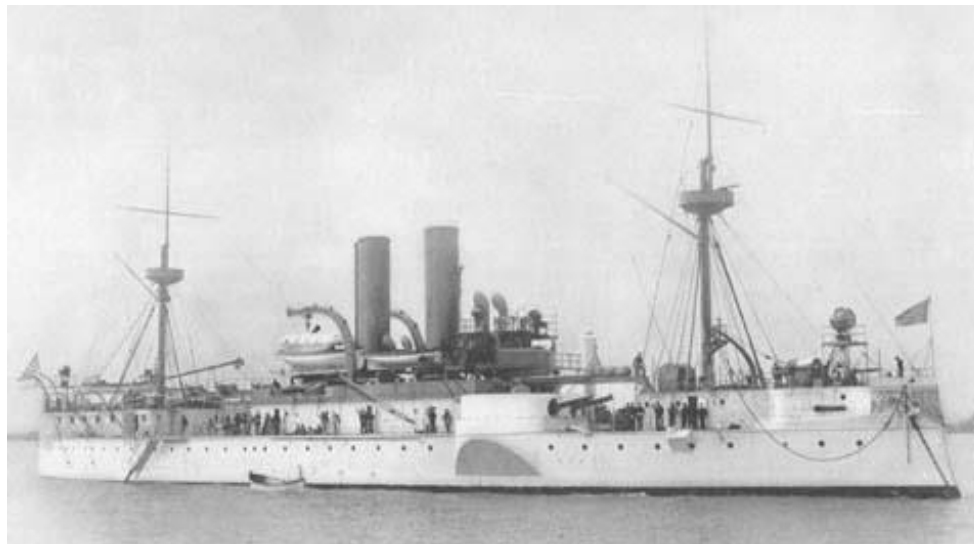
Date Written: January 31, 2018

POPULATION BASED

PRECISION BASED







To achieve great things, two things are needed:  
a plan, and not quite enough **time**.

Leonard Bernstein

Para **procesamiento de texto en historia clínica**: [ihmedrano@savanamed.com](mailto:ihmedrano@savanamed.com)



